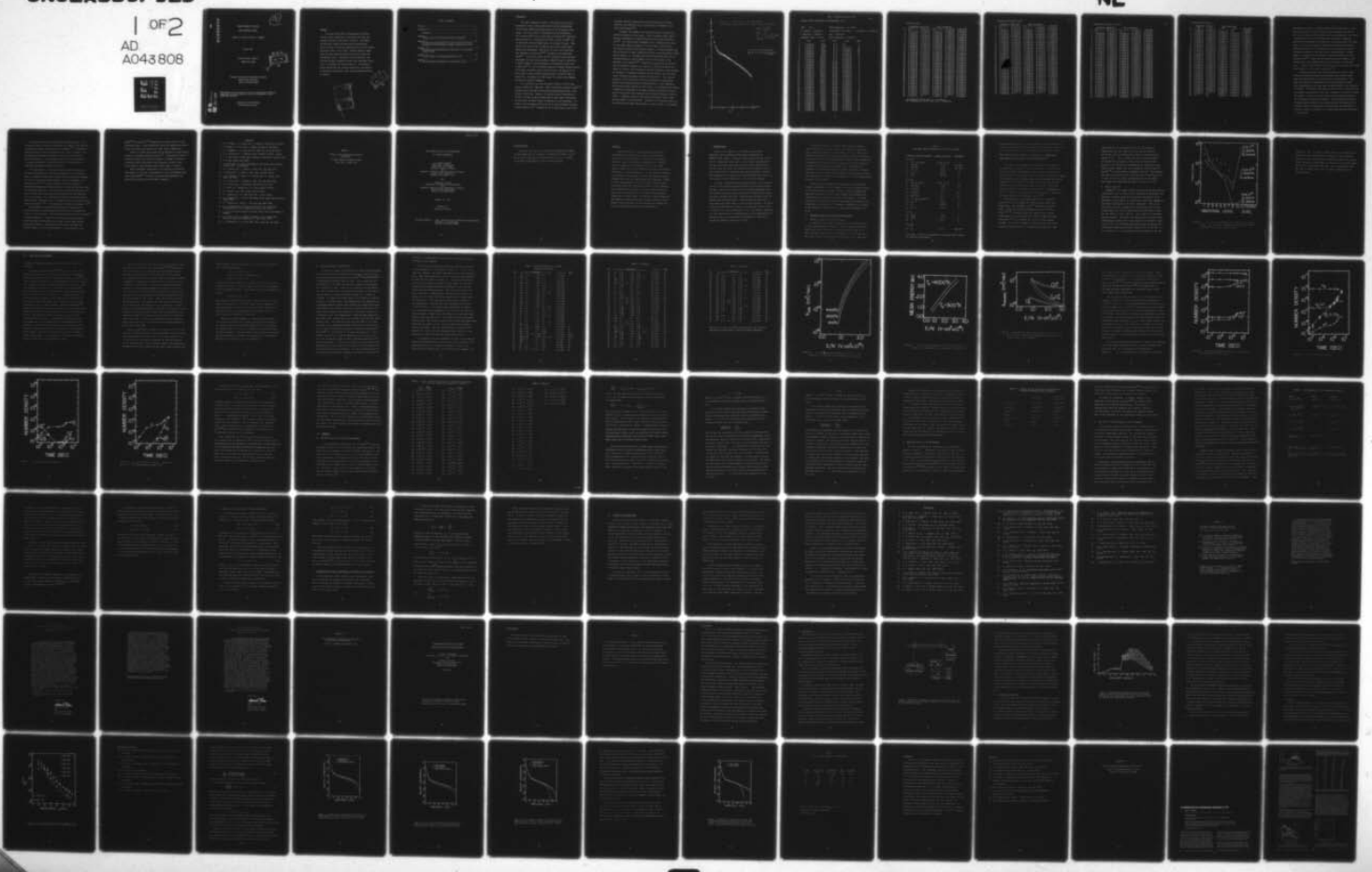
AD-A043 808 WAYNE STATE UNIV DETROIT MICH RESEARCH INST FOR ENGI--ETC F/G 20/5
ENERGY TRANSFER IN LASERS.(U)
JUN 77 E R FISHER, A J LIGHTMAN N00014-75-C-0284

UNCLASSIFIED NL

1 OF 2
AD
A043808



AD A043808

ENERGY TRANSFER IN LASERS

FINAL TECHNICAL REPORT

Edward R. Fisher and Allan J. Lightman

20 June 1977

DDC
RECEIVED
SEP 7 1977
C

Office of Naval Research

N00014-75-C-0284

Research Institute for Engineering Sciences
Wayne State University
Detroit, Michigan 48202

AD No. 1
DDC FILE COPY

The findings in this report are not to be construed as an official Department of the Navy position, unless so designated by other authorized documents.

Approved for Public Release
Distribution Unlimited

Abstract

This final report details plasma-chemical and energy transfer studies carried out at the Research Institute for Engineering Sciences, Wayne State University. Experimental and analytical research has been aimed at understanding additive effects in discharge supported molecular laser systems, particularly the CO laser system. Extensive numerical model codes have been developed and applied to the CO system with considerable success. Experiments in our laboratories have provided important information on high lying vibrational states in CO, in agreement with model predictions. Collaborative studies between RIES and Princeton University on the behavior of vibrational distributions under strongly pumped conditions is outlined.

DDC
SEP 7 1977



TABLE OF CONTENTS

Abstract i

Introduction 1

References 12

Appendix I 13
"Effects of O_2 on Low Pressure CO Laser Discharges"

Appendix II 63
Collaborative papers between RIES and Princeton University presented at 5th Conference on Chemical and Molecular Lasers

Appendix III 68
"CO Vibrational Distributions to High Levels in Low Pressure CO/He Mixtures"

Appendix IV 90
"A-Coefficients for Spontaneous Emission in CO"

Appendix V 94
"CO Vibrational Distributions in the Presence of O_2"

Introduction

This report summarizes research in the Research Institute for Engineering Sciences at Wayne State University into enhanced power and efficiency induced by additive species in the CO molecular laser system. This laser system is characterized by high efficiencies, 60% in pulsed mode[1] and up to 50% under CW conditions[2], significant power densities in a relatively small volume, of order 100 KW[3] and a rather broad lasing wavelength range, 4.8 to about 8 microns. These features are often a result of additive species which significantly improve laser performance. Many reviews of the CO laser system have been performed in recent years[4-6], including our own unpublished review[7]. In this final report, we will concentrate on the two major developments from our research program; a detailed study of the effects of additive gases on laser performance and collaborative studies with H. Rabitz and S. H. Lam at Princeton University on energy transfer processes in the upper vibrational states of the CO system. The majority of our work to date in these areas has appeared either in technical report or journal form, therefore, this final report will serve to draw together this work in a coherent framework.

It is justified to say that the general behavior of the CO laser system is rather well understood. Model calculations by several groups[8-13] have been able to adequately reproduce measured performance under a wide variety of conditions. However, a significant range of operating conditions in CO laser systems involves additive gases whose concentrations are quite small but whose effects are dominant on laser performance. For example, the high reported efficencies for CO laser performance involving Xe and Hg additives[14]. Although the role of these gases is very likely

to enhance ionization characteristics of CO-He and promote discharge stability, other additives such as O_2 and N_2 are not amenable to such simple interpretations[15].

In general, the interest in our studies has been to discharge supported low pressure CO laser systems. Thus, our modeling codes involved the early development of a non-equilibruim electron energy distribution code[16]. This code has been instrumental in our subsequent energy transfer and plasma chemistry studies as it has provided us with the basic input rates for modeling and simulation studies. It is worth remarking here that in molecular or atomic systems which exhibit strong metastability toward internal energy, i.e. vibrational and in which large energy densities are involved,superclastic energy feedback from the lasing species to the electrons is very important[15]. Superelastic processes are the reverse of electron excitation processes, i.e. reactions in which the electrons gain energy in collisions with vibrationally excited CO molecules. These processes are important in discharge environments when the molecular internal energy states (vibration) are highly excited as in the CO laser. Thus, electron processes in high vibrational states can be important as an energy loss mechanism even though the reverse excitation process is small compared to other energy transfer processes in these states. As an example of this effect, a demonstration calculation on the shape of the CO vibrational distribution both with and without upper vibrational state electron processes is shown in Figure 1. Conditions typical of low pressure CO discharge laser systems have been chosen in the calculation. The details of the numerical output for the calculation with upper state processes is given in Table I. By reference

Figure 1: Comparison of a CO vibrational distribution with and without upper state e-processes.

P_{total} = 8.5 torr
T = 155 K
CO/He = 1/7
E/N = 1.5×10^{-16} V-cm^2
$e_{density}$ = 2×10^{10}/cc

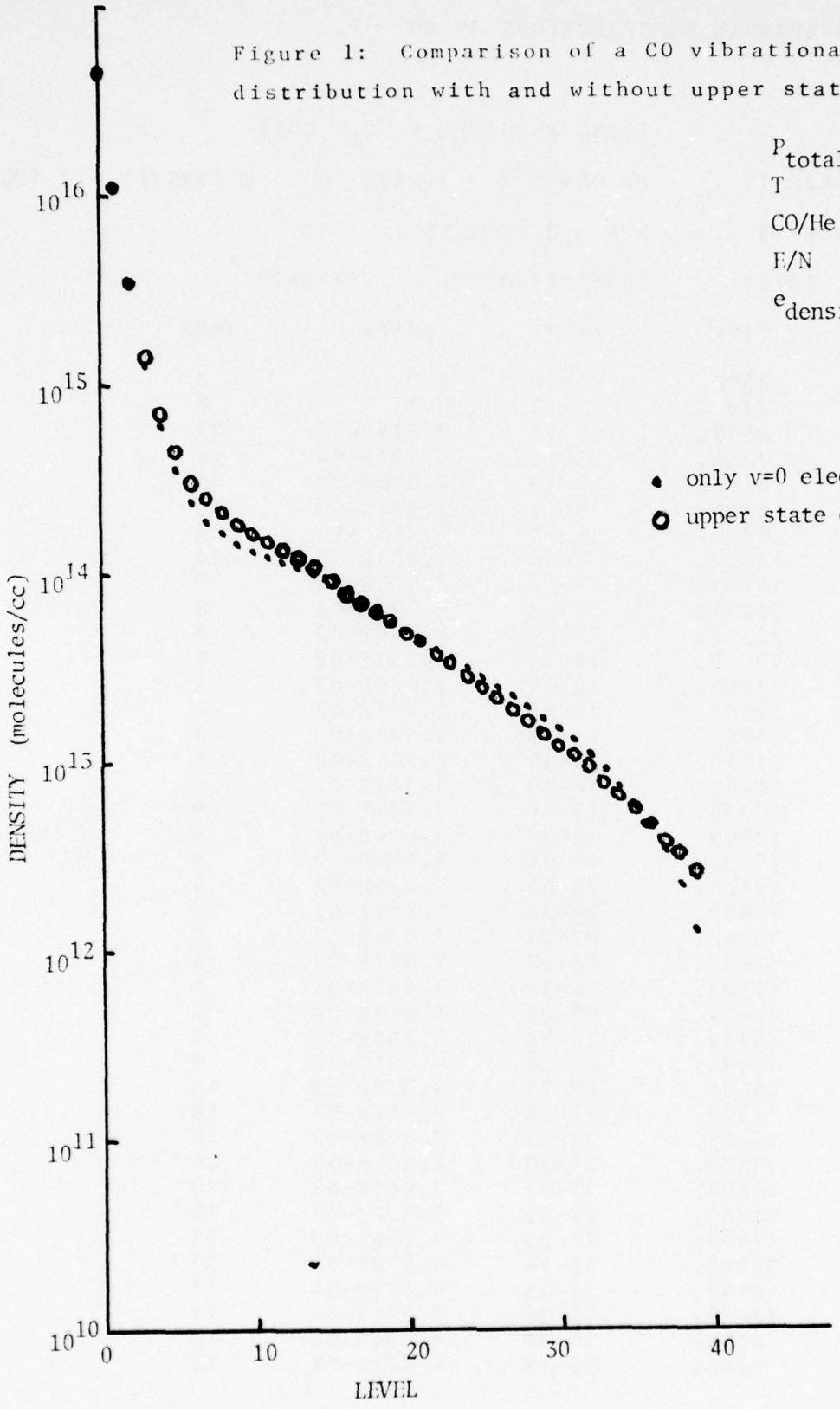


Table I: Steady State Rates in CO

STEADY STATE VIBRATIONAL DISTRIBUTIONS IN CO

TEMP = 155.K TOTAL PRESSURE = 8.5 TORR

CC DENSITY = 0.662E+17 HE DENSITY = 0.463E+18 O DENSITY = 0.100E+06

E DENSITY = 0.200E+11 E/N = 0.150E-15

ELECTRON TEMP = 13793. DRIFT VELOCITY = 0.371E+07

V	C(V)	T(V)	V-V*	GAIN	JMAX
0	4.648E+16	2500.	0- 0	0.0	0
1	1.135E+16	2189.	1- 0	0.0	0
2	3.541E+15	2617.	2- 1	7.214E-08	29
3	1.406E+15	3258.	3- 2	6.323E-06	24
4	7.028E+14	4288.	4- 3	2.085E-04	19
5	4.308E+14	5995.	5- 4	2.284E-03	15
6	3.092E+14	8730.	6- 5	9.208E-03	11
7	2.461E+14	12537.	7- 6	1.801E-02	10
8	2.079E+14	16741.	8- 7	2.405E-02	9
9	1.812E+14	20231.	9- 8	2.750E-02	8
10	1.602E+14	22274.	10- 9	2.838E-02	8
11	1.424E+14	23057.	11-10	2.790E-02	8
12	1.268E+14	23000.	12-11	2.663E-02	8
13	1.128E+14	22501.	13-12	2.493E-02	8
14	1.002E+14	21953.	14-13	2.338E-02	8
15	8.885E+13	21319.	15-14	2.146E-02	8
16	7.870E+13	20812.	16-15	1.963E-02	8
17	6.963E+13	20336.	17-16	1.792E-02	9
18	6.156E+13	19909.	18-17	1.634E-02	9
19	5.442E+13	19603.	19-18	1.489E-02	9
20	4.805E+13	19108.	20-19	1.326E-02	9
21	4.238E+13	18657.	21-20	1.177E-02	9
22	3.730E+13	18082.	22-21	1.034E-02	9
23	3.279E+13	17653.	23-22	9.083E-03	9
24	2.880E+13	17223.	24-23	7.941E-03	9
25	2.523E+13	16653.	25-24	6.857E-03	9
26	2.206E+13	16114.	26-25	5.890E-03	9
27	1.922E+13	15474.	27-26	4.991E-03	9
28	1.673E+13	15071.	28-27	4.277E-03	10
29	1.450E+13	14437.	29-28	3.604E-03	10
30	1.253E+13	13875.	30-29	2.878E-03	10
31	1.077E+13	13179.	31-30	2.364E-03	10
32	9.182E+12	12224.	32-31	1.869E-03	10
33	7.811E+12	11883.	33-32	1.542E-03	10
34	6.623E+12	11435.	34-33	1.256E-03	11
35	5.596E+12	10983.	35-34	1.022E-03	11
36	4.714E+12	10590.	36-35	8.307E-04	11
37	3.986E+12	10619.	37-36	7.071E-04	11
38	3.265E+12	8758.	38-37	4.524E-04	12
39	2.709E+12	9166.	39-38	4.021E-04	12

ELECTRON RATES

V	FORMATION PROCESSES (V-L) TO V	FORMATION PROCESSES (V+L) TO V	LOSS PROCESSES V TO (V-L)	LOSS PROCESSES V TO (V+L)	NET RATE
0	0.0	0.246E+19	0.0	0.856E+19	-0.610E+19
1	0.557E+19	0.165E+19	0.206E+19	0.418E+19	0.978E+18
2	0.416E+19	0.108E+19	0.156E+19	0.196E+19	0.172E+19
3	0.265E+19	0.803E+18	0.106E+19	0.104E+19	0.136E+19
4	0.173E+19	0.677E+18	0.776E+18	0.647E+18	0.983E+18
5	0.116E+19	0.624E+18	0.639E+18	0.476E+18	0.664E+18
6	0.859E+18	0.603E+18	0.584E+18	0.399E+18	0.480E+18
7	0.650E+18	0.595E+18	0.568E+18	0.363E+18	0.314E+18
8	0.498E+18	0.588E+18	0.569E+18	0.345E+18	0.172E+18
9	0.405E+18	0.579E+18	0.573E+18	0.334E+18	0.779E+17
10	0.362E+18	0.566E+18	0.574E+18	0.325E+18	0.292E+17
11	0.339E+18	0.549E+18	0.571E+18	0.315E+18	0.257E+16
12	0.325E+18	0.529E+18	0.563E+18	0.304E+18	-0.131E+17
13	0.312E+18	0.505E+18	0.548E+18	0.291E+18	-0.223E+17
14	0.300E+18	0.479E+18	0.530E+18	0.277E+18	-0.280E+17
15	0.286E+18	0.452E+18	0.508E+18	0.262E+18	-0.311E+17
16	0.272E+18	0.425E+18	0.483E+18	0.246E+18	-0.328E+17
17	0.257E+18	0.397E+18	0.457E+18	0.231E+18	-0.336E+17
18	0.242E+18	0.370E+18	0.430E+18	0.215E+18	-0.338E+17
19	0.227E+18	0.343E+18	0.404E+18	0.201E+18	-0.341E+17
20	0.212E+18	0.317E+18	0.377E+18	0.186E+18	-0.337E+17
21	0.197E+18	0.292E+18	0.350E+18	0.172E+18	-0.332E+17
22	0.182E+18	0.268E+18	0.324E+18	0.158E+18	-0.320E+17
23	0.168E+18	0.245E+18	0.299E+18	0.145E+18	-0.308E+17
24	0.155E+18	0.223E+18	0.275E+18	0.133E+18	-0.298E+17
25	0.142E+18	0.202E+18	0.252E+18	0.121E+18	-0.284E+17
26	0.130E+18	0.182E+18	0.229E+18	0.110E+18	-0.271E+17
27	0.118E+18	0.163E+18	0.208E+18	0.991E+17	-0.253E+17
28	0.107E+18	0.146E+18	0.188E+18	0.894E+17	-0.241E+17
29	0.971E+17	0.130E+18	0.169E+18	0.801E+17	-0.225E+17
30	0.874E+17	0.115E+18	0.152E+18	0.716E+17	-0.211E+17
31	0.784E+17	0.101E+18	0.135E+18	0.635E+17	-0.196E+17
32	0.699E+17	0.875E+17	0.119E+18	0.557E+17	-0.172E+17
33	0.618E+17	0.748E+17	0.104E+18	0.483E+17	-0.161E+17
34	0.545E+17	0.629E+17	0.914E+17	0.414E+17	-0.154E+17
35	0.478E+17	0.521E+17	0.796E+17	0.350E+17	-0.148E+17
36	0.417E+17	0.414E+17	0.691E+17	0.288E+17	-0.147E+17
37	0.363E+17	0.305E+17	0.601E+17	0.228E+17	-0.162E+17
38	0.315E+17	0.192E+17	0.506E+17	0.153E+17	-0.152E+17
39	0.269E+17	0.0	0.431E+17	0.0	-0.162E+17

NET ELECTRON ENERGY INTO CO = 4.871E+22
NET SUPERELASTIC ENERGY OUT OF CO =-2.960E+22

VIBRATION-VIBRATION RATES

V	FORMATION PROCESSES (V-1) TO V	FORMATION PROCESSES (V+1) TO V	LOSS PROCESSES V TO (V-1)	LOSS PROCESSES V TO (V+1)	NET RATE
0	0.0	0.747E+21	0.0	0.742E+21	0.570E+19
1	0.729E+21	0.742E+21	0.747E+21	0.724E+21	-0.839E+18
2	0.400E+21	0.724E+21	0.729E+21	0.397E+21	-0.163E+19
3	0.178E+21	0.397E+21	0.400E+21	0.176E+21	-0.131E+19
4	0.817E+20	0.176E+21	0.178E+21	0.808E+20	-0.968E+18
5	0.449E+20	0.808E+20	0.817E+20	0.446E+20	-0.660E+18
6	0.301E+20	0.446E+20	0.449E+20	0.303E+20	-0.488E+18
7	0.232E+20	0.303E+20	0.301E+20	0.237E+20	-0.322E+18
8	0.197E+20	0.237E+20	0.232E+20	0.204E+20	-0.189E+18
9	0.175E+20	0.204E+20	0.197E+20	0.183E+20	-0.950E+17
10	0.159E+20	0.183E+20	0.175E+20	0.168E+20	-0.488E+17
11	0.146E+20	0.168E+20	0.159E+20	0.155E+20	-0.170E+17
12	0.134E+20	0.155E+20	0.146E+20	0.143E+20	-0.692E+16
13	0.123E+20	0.143E+20	0.134E+20	0.132E+20	-0.136E+16
14	0.112E+20	0.132E+20	0.123E+20	0.121E+20	0.819E+16
15	0.102E+20	0.121E+20	0.112E+20	0.111E+20	0.155E+17
16	0.925E+19	0.111E+20	0.102E+20	0.101E+20	0.226E+17
17	0.837E+19	0.101E+20	0.925E+19	0.917E+19	0.280E+17
18	0.756E+19	0.917E+19	0.837E+19	0.834E+19	0.320E+17
19	0.681E+19	0.834E+19	0.756E+19	0.756E+19	0.258E+17
20	0.613E+19	0.756E+19	0.681E+19	0.684E+19	0.303E+17
21	0.5[illegible]19	0.684E+19	0.613E+19	0.619E+19	0.260E+17
22	0.[illegible]+19	0.619E+19	0.550E+19	0.558E+19	0.335E+17
23	0[illegible]19	0.558E+19	0.493E+19	0.503E+19	0.324E+17
24	[illegible]3E+19	0.503E+19	0.441E+19	0.453E+19	0.265E+17
25	0.349E+19	0.453E+19	0.393E+19	0.406E+19	0.276E+17
26	0.309E+19	0.406E+19	0.349E+19	0.363E+19	0.243E+17
27	0.272E+19	0.363E+19	0.309E+19	0.323E+19	0.317E+17
28	0.237E+19	0.323E+19	0.272E+19	0.286E+19	0.236E+17
29	0.206E+19	0.286E+19	0.237E+19	0.253E+19	0.247E+17
30	0.177E+19	0.253E+19	0.206E+19	0.222E+19	0.201E+17
31	0.150E+19	0.222E+19	0.177E+19	0.193E+19	0.143E+17
32	0.125E+19	0.193E+19	0.150E+19	0.166E+19	0.277E+17
33	0.103E+19	0.166E+19	0.125E+19	0.141E+19	0.215E+17
34	0.828E+18	0.141E+19	0.103E+19	0.119E+19	0.184E+17
35	0.645E+18	0.119E+19	0.828E+18	0.991E+18	0.173E+17
36	0.480E+18	0.991E+18	0.645E+18	0.805E+18	0.217E+17
37	0.396E+18	0.805E+18	0.480E+18	0.700E+18	0.213E+17
38	0.296E+18	0.700E+18	0.396E+18	0.587E+18	0.125E+17
39	0.587E+18	0.0	0.296E+18	0.0	0.291E+18

VIBRATION-TRANSLATION RATES

V	FORMATION PROCESSES (V-1) TO V	FORMATION PROCESSES (V+1) TO V	LOSS PROCESSES V TO (V-1)	LOSS PROCESSES V TO (V+1)	NET RATE
0	0.0	0.167E+17	0.0	0.156E+09	0.167E+17
1	0.156E+09	0.287E+17	0.167E+17	0.270E+09	0.121E+17
2	0.270E+09	0.327E+17	0.287E+17	0.308E+09	0.394E+16
3	0.308E+09	0.325E+17	0.327E+17	0.311E+09	-0.147E+15
4	0.311E+09	0.395E+17	0.325E+17	0.392E+09	0.693E+16
5	0.392E+09	0.456E+17	0.395E+17	0.493E+09	0.611E+16
6	0.493E+09	0.588E+17	0.456E+17	0.731E+09	0.132E+17
7	0.731E+09	0.694E+17	0.588E+17	0.104E+10	0.106E+17
8	0.104E+10	0.881E+17	0.694E+17	0.162E+10	0.187E+17
9	0.162E+10	0.107E+18	0.881E+17	0.246E+10	0.186E+17
10	0.246E+10	0.128E+18	0.107E+18	0.373E+10	0.212E+17
11	0.373E+10	0.144E+18	0.128E+18	0.534E+10	0.165E+17
12	0.534E+10	0.167E+18	0.144E+18	0.783E+10	0.222E+17
13	0.783E+10	0.193E+18	0.167E+18	0.115E+11	0.260E+17
14	0.115E+11	0.215E+18	0.193E+18	0.163E+11	0.224E+17
15	0.163E+11	0.233E+18	0.215E+18	0.224E+11	0.181E+17
16	0.224E+11	0.246E+18	0.233E+18	0.299E+11	0.127E+17
17	0.299E+11	0.254E+18	0.246E+18	0.391E+11	0.803E+16
18	0.391E+11	0.258E+18	0.254E+18	0.502E+11	0.416E+16
19	0.502E+11	0.269E+18	0.258E+18	0.660E+11	0.105E+17
20	0.660E+11	0.274E+18	0.269E+18	0.850E+11	0.560E+16
21	0.850E+11	0.283E+18	0.274E+18	0.111E+12	0.926E+16
22	0.111E+12	0.284E+18	0.283E+18	0.140E+12	0.483E+15
23	0.140E+12	0.284E+18	0.284E+18	0.177E+12	0.170E+15
24	0.177E+12	0.289E+18	0.284E+18	0.227E+12	0.499E+16
25	0.227E+12	0.292E+18	0.289E+18	0.288E+12	0.249E+16
26	0.288E+12	0.296E+18	0.292E+18	0.368E+12	0.432E+16
27	0.368E+12	0.291E+18	0.296E+18	0.454E+12	-0.501E+16
28	0.454E+12	0.293E+18	0.291E+18	0.575E+12	0.192E+16
29	0.575E+12	0.292E+18	0.293E+18	0.722E+12	-0.493E+15
30	0.722E+12	0.294E+18	0.292E+18	0.916E+12	0.206E+16
31	0.916E+12	0.301E+18	0.294E+18	0.118E+13	0.618E+16
32	0.118E+13	0.291E+18	0.301E+18	0.143E+13	-0.974E+16
33	0.143E+13	0.286E+18	0.291E+18	0.177E+13	-0.475E+16
34	0.177E+13	0.284E+18	0.286E+18	0.220E+13	-0.253E+16
35	0.220E+13	0.282E+18	0.284E+18	0.274E+13	-0.203E+16
36	0.274E+13	0.275E+18	0.282E+18	0.334E+13	-0.654E+16
37	0.334E+13	0.270E+18	0.275E+18	0.423E+13	-0.478E+16
38	0.423E+13	0.274E+18	0.270E+18	0.531E+13	0.414E+16
39	0.531E+13	0.0	0.274E+18	0.0	-0.274E+18

RADIATIVE PROCESSES

V	FORMATION PROCESSES FUN	FORMATION PROCESSES OVER	LOSS PROCESSES FUN	LOSS PROCESSES OVER	NET RATE
0	0.381E+18	0.305E+16	0.0	0.0	0.384E+18
1	0.228E+18	0.361E+16	0.381E+18	0.0	-0.149E+18
2	0.130E+18	0.357E+16	0.228E+18	0.305E+16	-0.915E+17
3	0.831E+17	0.361E+16	0.130E+18	0.361E+16	-0.400E+17
4	0.609E+17	0.386E+16	0.831E+17	0.357E+16	-0.148E+17
5	0.502E+17	0.426E+16	0.609E+17	0.361E+16	-0.290E+16
6	0.444E+17	0.474E+16	0.502E+17	0.386E+16	0.284E+16
7	0.410E+17	0.526E+16	0.444E+17	0.426E+16	0.612E+16
8	0.383E+17	0.574E+16	0.410E+17	0.474E+16	0.777E+16
9	0.359E+17	0.614E+16	0.383E+17	0.526E+16	0.900E+16
10	0.335E+17	0.647E+16	0.359E+17	0.574E+16	0.981E+16
11	0.309E+17	0.672E+16	0.335E+17	0.614E+16	0.103E+17
12	0.282E+17	0.688E+16	0.309E+17	0.647E+16	0.107E+17
13	0.257E+17	0.688E+16	0.282E+17	0.672E+16	0.110E+17
14	0.231E+17	0.684E+16	0.257E+17	0.688E+16	0.111E+17
15	0.207E+17	0.677E+16	0.231E+17	0.688E+16	0.113E+17
16	0.184E+17	0.663E+16	0.207E+17	0.684E+16	0.112E+17
17	0.163E+17	0.642E+16	0.184E+17	0.677E+16	0.111E+17
18	0.143E+17	0.621E+16	0.163E+17	0.663E+16	0.109E+17
19	0.125E+17	0.591E+16	0.143E+17	0.642E+16	0.105E+17
20	0.109E+17	0.562E+16	0.125E+17	0.621E+16	0.102E+17
21	0.946E+16	0.528E+16	0.109E+17	0.591E+16	0.974E+16
22	0.810E+16	0.496E+16	0.946E+16	0.562E+16	0.922E+16
23	0.694E+16	0.463E+16	0.810E+16	0.528E+16	0.875E+16
24	0.592E+16	0.427E+16	0.694E+16	0.496E+16	0.821E+16
25	0.500E+16	0.391E+16	0.592E+16	0.463E+16	0.761E+16
26	0.419E+16	0.354E+16	0.500E+16	0.427E+16	0.701E+16
27	0.350E+16	0.318E+16	0.419E+16	0.391E+16	0.639E+16
28	0.289E+16	0.270E+16	0.350E+16	0.354E+16	0.563E+16
29	0.211E+16	0.232E+16	0.289E+16	0.318E+16	0.472E+16
30	0.181E+16	0.198E+16	0.211E+16	0.270E+16	0.438E+16
31	0.154E+16	0.168E+16	0.181E+16	0.232E+16	0.373E+16
32	0.131E+16	0.143E+16	0.154E+16	0.198E+16	0.317E+16
33	0.111E+16	0.120E+16	0.131E+16	0.168E+16	0.269E+16
34	0.940E+15	0.101E+16	0.111E+16	0.143E+16	0.227E+16
35	0.792E+15	0.858E+15	0.940E+15	0.120E+16	0.191E+16
36	0.670E+15	0.703E+15	0.792E+15	0.101E+16	0.160E+16
37	0.548E+15	0.584E+15	0.670E+15	0.858E+15	0.132E+16
38	0.455E+15	0.0	0.548E+15	0.703E+15	-0.796E+15
39	0.0	0.0	0.455E+15	0.584E+15	-0.104E+16

the second page of Table I, labeled "electron rates" we note that in vibrational states above v=11 the net electron rates are negative indicating a net flow of energy from the vibrational levels to the electrons. This feature is characteristic of all of our distribution calculations although the quantitative rates depends on the particular cross sections used in the upper states. Also in the CO system our studies have indicated that electronic excitation by electrons is important both for plasma heating as a result of subsequent quenching collisions but also for carbon formation. Although carbon is not predicted to be important in the plasma chemistry of the CO discharge laser[15], it does limit the operating time due to deposits which increase cavity losses leading eventually to a reduction in lasing power output. Therefore, the electronic cross sections which are rather poorly known become important in large scale CO predictions[15].

In modeling the dynamic and steady state behavior of the CO system we have also developed and applied time dependent and CW codes incorporating stimulated emission and state-of-the-art rate coefficients. These codes have enabled our understanding of CO laser performance to become quite sophisticated in those cases where the basic molecular rate information is available. In addition, these model calculations have indicated priorities on important rate processes for which poor information is currently available. Our studies on O_2 effects in the CO laser plasma and subsequent effects on laser performance as detailed in Appendix I have indicated the importance of plasma chemistry effects in low pressure molecular discharges and reinforced the need for continued work in providing basic rate information on molecular systems as a precurson to our understanding and hence optimization of laser systems.

Our understanding of the detailed energy transfer processes in the CO system was given a significant contribution as a result of the vibration-translation calculations on CO-He by Verter and Rabitz[17]. Collaboration between the groups in RIES and Princeton led to a series of papers at the 5th Conference on Chemical and Molecular lasers in St. Louis in April (1977)-see Appendix II. The collaboration was particularly successful as it blended the theoretical and analytical effort at Princeton with the experimental and modeling capabilities in RIES.

It has been known for a long time that energy transfer processes in the upper vibrational states of CO play an important role in CO laser behavior. Substantial output power is emitted from vibrational states between $v \simeq 10$ and $v \simeq 15$ while even higher vibrational states are important in the dissociation of CO[15]. Yet until recently, no direct calculation or experimental measurements have been available to incorporate into laser codes for performance predictions. The Verter-Rabitz calculations provided for the first time some sound calculations on the temperature and level dependence of VT rates in CO-He. It is significant to note that large deviations were noted for upper vibrational levels, i.e. above about v=30, from the previously accepted SSH results[17-18]. These conclusions are detailed in Appendix III[18].

The experimental technique developed during this program involves direct observation of the spontaneous end-light emission on overtone transitions in a CO laser plasma. The original work within RIES on this technique[21] is given in Appendix IV. Currently, we are able to observe and interpret the CO vibrational distribution up to v=35 under varying plasma chemical and physical conditons. The observation of the entire vibrational distribution through the second "knee" provides a unique comparison to both

model[18] and analytical[19] interpretations of energy transfer in high vibrational levels. These collaborative studies are continuing to provide insight into other gase mixtures, and a wider range of temperatures.

Lastly, our studies have pointed out the importance of plasma-chemical processes in discharge supported CO lasers[15]. These extensive model calculations suggested that rather small amoun ts of O-atoms, particularly produced by direct dissociation of O_2 by electrons, can have a detrimental effect on laser performance due to upper state V-T processes.

Recent experimental measurements in our laboratory on vibrational distributions in a CO laser in the presence of O_2 have collaborated these model calculations[20]. The report discribing these measurements and detailing the conclusions can be formed in Appendix V.

References

1. M. J. Plummer, J. L. Wagner and W. J. Glowacki, IEEE JQE 11, 700 (1975).
2. M. M. Mann, D. K. Rice and R. G. Eguchi, IEEE JQE 10, 682 (1974).
3. M. L. Bhaumick, W. B. Lacina and M. M. Mann, IEEE JQE 8, 682 (1972).
4. N. N. Sobolev and V. V. Sokouiko, Kvant. Elektron. No.4(10), 3 (1972).
5. C. C. Chen, Report P-5163, Rand Corporation, Santa Monica, January (1974).
6. M. M. Mann, AIAA 5, 549 (1976).
7. S. W. Kim and E. R. Fisher, RIES Report 77-120, Wayne State University, January (1977) (unpublished).
8. W. Q. Jeffers and C. E. Wiswall, J. Appl. Phys. 42, 5059 (1971).
9. G. Abraham and E. R. Fisher, J. Appl. Phys. 43, 4621 (1972).
10. S. D. Rockwood. J. E. Brau, W. A. Proctor and G. H. Canavan, IEEE JQE 9, 120 (1973).
11. R. E. Center and G. E. Caledonia J. Appl. Phys. 46, 2215 (1975).
12. W. B. Lacina and G. L. McAllister, IEEE JQE 11, 235 (1975).
13. J. W. Rich, R. C. Bergman and J. A. Lordi, AIAA 13, 95 (1975).
14. M. L. Bhaumik, Appl. Phys. Letters 17, 188 (1970).
15. W. L. Morgan and E. R. Fisher, Phys. Rev., in press (1977).
16. W. L. Morgan and E. R. Fisher, RIES Report 74-56, Wayne State University, August (1974).
17. M. R. Verter and H. Rabitz, J. Chem. Phys. 64, 2929 (1976).
18. A. J. Lightman and E. R. Fisher, RIES Report 77-121, Wayne State University, April (1977) submitted to J. Appl. Phys. (1977).
19. S. H. Lam, Princeton University, preprint, March (1977); see Appendix II attached.
20. E. R. Fisher and A. J. Lightman, RIES Report 77-122, Wayne State University, June (1977) submitted to J. Chem. Phys. (1977).
21. A. J. Lightman and E. R. Fisher, Appl. Phys. Letters 29, 593 (1976).

Appendix I

"Effects of O_2 on Low Pressure CO Laser Discharges"

W.Lowell Morgan and Edward R.Fisher

Phys. Rev., in press 1977

THE EFFECTS OF O_2 ON LOW-PRESSURE CO LASER DISCHARGES

W. Lowell Morgan*
Department of Physics
University of Windsor
Windsor, Ontario, Canada
and
Research Institute for Engineering Sciences
Wayne State University
Detroit, Michigan U.S.A.

and

Edward R. Fisher
Department of Chemical Engineering
and
Research Institute for Engineering Sciences
Wayne State University
Detroit, Michigan 48202

January 31, 1977

Submitted to
Physical Reviews

*Present Address: Joint Institute for Laboratory Astrophysics
University of Colorada
Boulder, Colorado 80302

ACKNOWLEDGMENT

The major part of this research was supported by DARPA through ONR-Boston on contract no. N00014-75-C-0284. W.L.M. would like to express his appreciation to Dr. A. V. Phelps for helpful discussions on part of this research.

ABSTRACT

Trace additions of several gases are known to significantly effect CO laser power and efficiency. Since small concentrations of additives are generally involved, these additives are recognized as predominantly influencing the characteristics of the laser plasma. Oxygen has been an additive receiving substantial attention in past measurements. In this paper we develop a consistent interpretation for all the observed oxygen effects both from our laboratories and elsewhere. Oxygen in small concentrations will be shown to improve laser efficiency and power through its effect on the electron-ion recombinations process. At higher oxygen additions, laser output is degraded due to vibration-translation relaxation by oxygen atoms. In addition, carbon formation and removal, plasma heating and cooling effects, heterogeneous loss processes and the influence of polymer ions will be discussed through model calculations.

I. INTRODUCTION

Oxygen as an additive in discharge sustained CO molecular laser systems has been used extensively to improve laser output. Although numerous observations on the role of oxygen have been made, no consistent interpretation has been developed which characterizes these observations. In this paper we review the observations on oxygen as an additive and present a detailed model which provides a consistent framework for interpreting these observations as well as the effects of other additives in the CO laser system.

In order to accomplish this understanding, the characteristics of the electron energy distribution have been studied through a numerical solution to the relevant Boltzmann equation and the detailed plasma and neutral chemistry and energy transfer processes have been characterized through a time dependent rate equation model. These models are detailed in this paper with application to the $CO/O_2/He$ system. Two major points are indicated as a result of this study on the effect of oxygen on CO laser performance: ionic and neutral chemistry are very important to an understanding of the observations on oxygen effects, and superelastic processes are critical to explaining observed ionization levels.

A uniform feature of additive gases found to enhance laser power and efficiency is the fact that these gases have lower ionization potentials than either CO or He. Thus, the additive can generally be viewed as being a source of electrons at an E/N (electric field/total number density) more appropriate to maintaining the mean electron energy near that for optimum coupling to the vibrational states of CO. Although this viewpoint is undoubtedly correct for some additives of general interest, e.g. Xe, oxygen will be shown to enhance laser output and efficiency as a result of its effect on the ion recombination dynamics in the plasma.

In this paper, homogeneous plasma chemistry and energy transfer processes will be stressed. At total pressures around 10 torr under liquid nitrogen cooling, it will be shown that ambipolar diffusion competes about equally with homogeneous recombination as the major electron loss process. At higher pressures, the electron density is dominated by ionization and homogeneous recombination. Attachment processes will be shown to be generally unimportant due to the large detachment rate by CO.

II. ELECTRON ENERGY DISTRIBUTION CALCULATIONS

A. Electron Impact Cross Section Data.

A summary of the electron impact cross section data used in this study appears in Table 1. Special mention should be made of the cross sections for electronic excitation of CO. Near threshold there is little information on the magnitude of the cross section for electronic excitation in CO. Most pre-

TABLE 1

ELECTRON IMPACT PROCESSES IN THE CO-O_2 SYSTEM

Electron Impact Processes	Energy Loss (eV)	Reference
$e^- + CO$:		
1. $CO^\dagger$ (8 levels)	0.266 - 2.034	2
2. $CO(a^3\Pi)$	6.04	see text
3. $CO(A^1\Pi)$	8.07	see text
4. $C + O^-$	9.00	3
5. $C^+ + O^-$	12.55	3
6. CO^+	14.013	4
$e^- + O_2$:		
7. $O_2^\dagger$ (8 levels)	0.193 - 1.46	4
8. $O_2(a^2\Delta_g)$	0.98	5
9. $O_2(b^1\Sigma_g^+)$	1.64	5
10. $O_2(A^3\Sigma_u^+)$	4.5	1,6
11. $O_2(B^3\Sigma_u^-)$	8.4	1,6
12. 9.7 eV allowed[9]	9.7	6
13. $O + O^-$	3.62	3
14. O_2^+	12.063	4
15. $O^+ + O$	19.54	3
$e^- + O$:		
16. $O(^1D)$	1.96	7
17. $O(^1S)$	4.17	7
18. O^+	13.6	4
$e^- + O_2^*$:		
19. O_2^+	11.0	see text

Note that † refers to vibrational excitation and * refers to electronic excitation.

vious workers have used a single composite cross section, due to Hake and Phelps,[1] with a threshold of 6 eV and a peak value of 5×10^{-16} cm^2 at 10 eV corresponding to the $CO(a^3\Pi)$ state. This cross section, however, is subject to considerable uncertainty as pointed out by Hake and Phelps.[1]

For total cross sections from threshold up to about 25 eV, the work of Ajello[8] on the excitation of $CO(a^3\Pi)$ and $CO(A^1\Pi)$ has been used together with the theoretical work of Chung and Lin[9] on the excitation of eleven CO electronic states. In the calculations reported here we have included the two CO electronic states with the largest cross sections: the $a^3\Pi$ state at 6.04 eV and the $A^1\Pi$ state at 8.07 eV. The cross sections used are composites of those given in References 8 and 9. They are in substantial agreement with a similar set of cross sections due to Sawada, et al.[10]

With reference to the exciting of the $A^3\Sigma$ and $B^3\Sigma$ states of O_2, it is known that these excited states predissociate. The $O_2(A^3\Sigma_u^+)$ state[11] predissociates into $O(^3P) + O(^3P)$ and $O_2(B^3\Sigma_u^-)$ predissociates into $O(^3P) + O(^1D)$.[11,12] Although there are several ways for the $O_2(B)$ state to predissociate into $O(^3P) + O(^3P)$ via curve crossings,[12] the probabilities of this occurring are unknown. It has been assumed in this work that all of the excitation follows the $^3P + {}^1D$ predissociative path. The

cross section for ionization of the O_2^* metastable is unknown and has been taken to be the same as that for ionization of $O_2(X)$ displaced in energy by the excitation energy of O_2^*. This is about the least arbitrary method of obtaining an estimate of the cross section for this process in the absence of experimental or theoretical data. There is some support for this assumption from the work of Burrow[13] on dissociative attachment from O_2^*. He measured the ratio of the ionization cross section of the $a^1\Delta_g$ state to that of the $X^3\Sigma_g$ state at approximately 0.5 eV above each respective threshold and found it to be 0.8 ± 0.3.

B. Results for CO.

Nighan[14] has shown through electron energy distribution calculations that as the E/N of a discharge is increased, the fraction of energy going into electronic excitation of CO increases at the expense of vibrational excitation suggesting that laser operation at low E/N is desirable. This is illustrated in Figure 1 which plots the fraction of electron energy going into the CO vibrational and electronics states for two values of E/N. Here $\bar{u}_r = 2/3\bar{u}$, where $\bar{u}$ is the mean electron energy. The effect of superelastic collisions with vibrationally excited CO is also shown in the Figure 1. Electrons in the 1-4 eV energy range gain quanta of energy from the excited vibrational states, ranging from .27 eV for v = 1 to 2.30 eV for v = 8, increasing the mean energy of the dis-

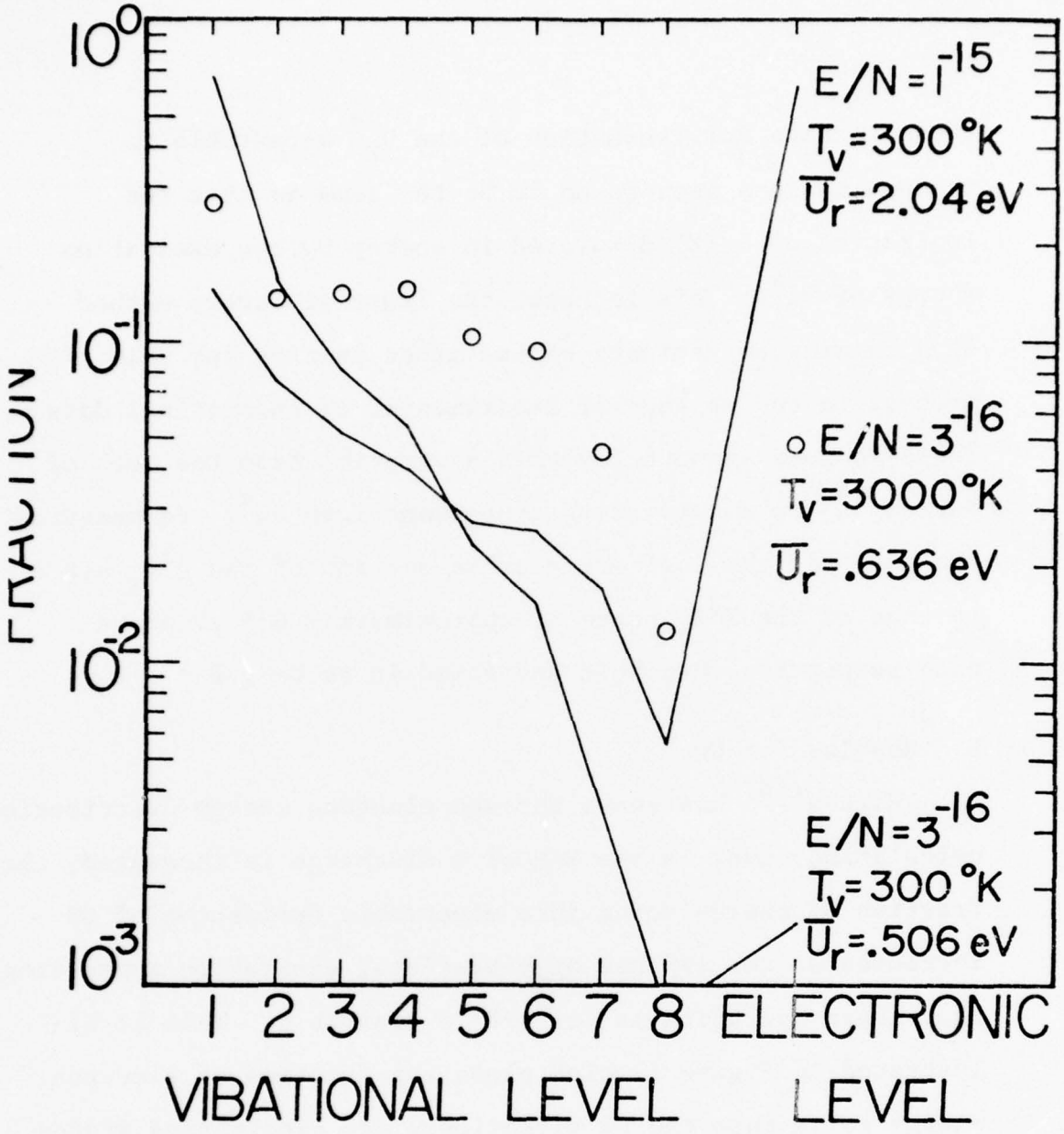


FIGURE 1: Fractional energy balance in pure CO as a function of E/N. The effect of including superelastic processes is demonstrated by the circled points.

tribution. This has only a slight effect on the vibrational excitation rate coefficients but dominates the electronic excitation and ionization rate coefficients due to the significant increase in the number of electrons in the high energy tail of the distribution function. This superelastic feedback will be shown later to be of great importance in CO laser operation.

III. THE CO-O_2-He DISCHARGE

A Review of Experimental Work on the Effects of O_2 on the CO Laser.

A number of experimenters[15-19] have found that a small amount of O_2 added to a CW CO laser plasma has a pronounced effect upon the operation of the laser. Bhaumik, et al[16] have found that small amounts of O_2 (approximately 5% of the CO partial pressure) enhanced the power output by a factor of 10-20% and reduced carbon deposits on the walls of the laser tube. They suggested that the O_2 affected the dissociation reaction $CO \rightleftarrows C + O$ by driving it to the left. Larger amounts of O_2 had a deleterious effect on laser operation, possibly due to the large electron attachment cross section of O_2 or to the formation of CO_2, in their opinion. Hartwick and Walder[17] found that the total laser output increased and that the laser became more stable with the addition of O_2 to the CO-He discharge. The optimum mixture was found to be 28 torr He, 2 torr CO and 0.1 torr O_2. In addition, they measured the gas temperature in the plasma using a thermocouple and correlated it to laser output finding that the minimum in temperature, approximately 295°K, corresponded to the maximum in power output as the O_2 flow rate was varied for a liquid nitrogen cooled laser. At slow oxygen flow rates the measured kinetic temperature was approximately 320°K.

Extensive work involving the effects of O_2 upon CO lasers has been done by Keren, Avivi and Dothan.[18,19] They found that the addition of O_2 increased the power output and decreased the operating E/N of a water cooled CO flow laser. At a constant current of 17 mA the laser output power reached a maximum of 4 watts with the addition of 50 m-torr of O_2 to a mixture of 1.4 torr CO in 18 torr He and the axial field strength in the discharge dropped from 136 V/cm to 88 V/cm. Power output then decreased with the addition of larger concentrations of O_2 and lasing was completely quenched at an O_2 partial pressure of 100 m-torr. They also pointed out that the discharge was very unstable and that laser action could not be obtained in the absence of the O_2 additive. On the basis of the measured decrease in E/N and a calculation of the fraction of electron energy flowing into CO vibrational and electronic states as a function of E/N (similar to that presented in Figure 1 here) they concluded that the enhanced power output was due to more efficient vibrational pumping because of the lower E/N.

Keren, et al[19] also analyzed the composition of the ions leaving the discharge using a mass spectrometer and found that with the addition of 20 m-torr O_2 to the laser plasma (1.4% of the CO partial pressure), O_2^+ became the dominant positive ion in the discharge. With no oxygen present the discharge was dominated by the $C_2O_2^+$ dimer ion and higher order polymer ions.

They suggested that the dominance of O_2^+ was due to ionization via a three step process:

$$e^- + CO \rightarrow CO^*(a^3) + e^-$$

$$CO^* + O_2 \rightarrow CO + O_2^* \text{ (metastable)}$$

$$O_2^* + e^- \rightarrow O_2^+ + 2e^-$$

claiming that the probability of producing O_2^+ by direct ionization is at least a factor of twenty lower than the probability of the above process. They dismiss the charge transfer reaction,

$$CO^+ + O_2 \rightarrow O_2^+ + CO$$

as a means of forming O_2^+ because, in their opinion, it cannot explain the decrease in E/N that occurs with the addition of molecular oxygen. Using this three step model, they compute that about 5% of the O_2 molecules are excited to O_2^* for a total O_2 partial pressure of 25 m-torr.

Because very small amounts of molecular oxygen added to a CO laser have significant effects upon laser performance, it appears clear that the plasma properties of the discharge are affected but, until now, a consistent interpretation has not been available. The calculations that follow are directed toward providing this systematic explanation of the observed properties of additive O_2 in a CO discharge.

B. Plasma Chemistry Calculations

In order to assess the importance of some of the processes that can occur in the discharge, the computer code for calculating the electron distribution function[20] was combined with a time-dependent chemical kinetics code. This allows the concentrations of all important chemical species to be computed as a function of time. Since we are studying CW laser behavior, this computation is carried out for times of the order of contact times in flowing CW laser systems (i.e., tenths of seconds). On these time scales many of the species concentrations are in steady state. The differential rate equations are integrated directly rather than solving the steady state equations because the coupled non-linear algebraic equations that arise from a steady state analysis are difficult to solve in a systematic way. More importantly, there are some species in a fast flow laser (such as CO_2 in a CO laser) that may not reach steady state. The chemistry code that was used in this work is based on the Runge-Kutta-Merson algorithm for the integration of stiff differential equations originally developed by Keneshea[21] in his studies of ionispheric chemistry. In this scheme, initial CO, O_2 and He densities and an initial electron and ion density close to their expected steady state values are specified. A value for E/N and an initial vibrational temperature are also specified as inputs to the calculation of the electron energy distribution. As time progresses and the CO vibrational temperature changes, the electron distribution

function is recomputed and new rate coefficients calculated to reflect these changes.

A list of the seventy-nine chemical reactions included in this calculation is presented in Table 2. Only a relative few, however, are really important and will be discussed here. The rate coefficients for the reactions and references to them are also given in Table 2. The rate coefficients for the first twenty reactions, except number (8), are computed using the electron energy distribution code and the cross sections discussed above. The rate coefficient used for ionization of vibrationally excited CO (reaction 8) is taken to be the same as that for ionization of ground state CO (reaction 5). The rate coefficients shown in Table 2 for reactions (1) through (20) were computed using an E/N = 1×10^{-16} V-cm^2 and a CO vibrational temperature of 3000°K for a gas mixture corresponding to 1.4 torr CO, 50 m-torr O_2 and 18 torr He. These values are shown for illustrative purposes as they are typical of the conditions being discussed in this work. The electron reduced mean energy ($\bar{u}_r$) under these conditions is about 1.0 eV. The gas temperature has been taken to be 300°K. The rate coefficients in reactions (21) through (79), where they are dependent upon electron or gas temperature, have been computed using these values.

To illustrate how the parameters critical to the calculations being presented here vary with E/N and vibrational temperatures, we have, in Figures 2 through 4 plots of the ionization rate coefficient of CO, mean electron energy, and

TABLE 2. Reactions Included in the Plasma Chemistry Calculations.

No.	Reactions	k	Ref.
1.	$CO + e = CO\dagger + e$	9.4 (-9)	
2.	$CO\dagger + e = CO + e$	2.2 (-8)	
3.	$CO + e = CO^* + e$	6.8 (-11)	
4.	$CO^* + e = CO + e$	1.6 (-8)	
5.	$CO + e = CO^+ + e + e$	2.4 (-14)	
6.	$CO + e = C + O^-$	2.8 (-14)	
7.	$CO + e = C^+ + O^- + e$	9.3 (-17)	
8.	$CO\dagger + e = CO^+ + e + e$	2.4 (-14)	
9.	$O_2 + e = O_2\dagger + e$	2.3 (-10)	
10.	$O_2\dagger + e = O_2 + e$	4.2 (-10)	
11.	$O_2 + e = O_2^* + e$	1.9 (-10)	
12.	$O_2^* + e = O_2 + e$	5.4 (-10)	
13.	$O_2 + e = O_2^+ + e + e$	6.6 (-14)	
14.	$O_2 + e = O + O + e$	5.1 (-11)	
15.	$O_2 + e = O + O^-$	5.5 (-12)	
16.	$O_2 + e = O^+ + O^- + e$	6.1 (-18)	
17.	$O_2 + e = O + O^* + e$	2.6 (-11)	
18.	$O + e = O^* + e$	6.1 (-10)	
19.	$O + e = O^+ + e + e$	4.9 (-14)	
20.	$O_2^* + e = O_2^+ + e + e$	1.6 (-13)	
21.	$O^- + CO = CO_2 + e$	7.3 (-10)	22
22.	$CO^* + CO = CO\dagger + CO\dagger$	9.9 (-11)	23
23.	$CO^* + CO = C + CO_2$	1.1 (-11)	23
24.	$CO^+ + CO + CO = C_2O_2^+ + CO$	1.4 (-28)	24-27
25.	$C_2O_2^+ + CO = CO^+ + CO + CO$	2.1 (-12)	24-27
26.	$C_2O_2^+ + e = CO + CO$	7.4 (-8)	28
27.	$O_2^+ + e = O + O$	1.0 (-8)	29
28.	$O_2^+ + e = O + O^*$	1.0 (-8)	29
29.	$O^* + O_2 = O + O_2$	7.5 (-11)	30
30.	$O_2 + O + M = O_3 + M$	6.4 (-34)	31

TABLE 2. (continued)

No.	Reactions	k	Ref.
31.	$O^* + O_3 = O_2 + O_2$	3.8 (-12)	30
32.	$O + O_3 = O_2 + O_2$	2.0 (-14)	31
33.	$O_2 + O_3 = O_2 + O_2 + O$	1.5 (-13)	31
34.	$O^+ + O_2 = O_2^+ + O$	4.0 (-11)	32
35.	$O_2^+ + e + M = O_2 + M$	8.0 (-29)	21
36.	$O^- + O_2^+ = O + O_2$	1.0 (-7)	33
37.	$O^- + O = O_2 + e$	2.0 (-10)	33
38.	$O^- + O_2 = O_3 + e$	5.0 (-15)	33
39.	$O_3 + e = O^- + O_2$	1.0 (-11)	33
40.	$O^- + O_2^* = O_3 + e$	3.0 (-10)	33
41.	$O^- + O_2^+ + M = O_3 + M$	1.9 (-27)	est.
42.	$O_2 + e + M = O_2^- + M$	1.0 (-33)	34
43.	$O + e + M = O^- + M$	1.0 (-31)	21
44.	$C + O_2 = CO^\dagger + O^*$	3.3 (-11)	35
45.	$C + CO_2 = CO + CO$	7.0 (-19)	35
46.	$C + O_2^\ddagger = CO^+ + O$	2.3 (-10)	35
47.	$C^+ + CO_2 = CO^+ + CO$	1.8 (-9)	32
48.	$C^+ + O_2 = CO^+ + O$	1.1 (-9)	32
49.	$CO^+ + e = C + O$	9.2 (-8)	35
50.	$CO^+ + e + M = CO + M$	8.5 (-27)	33
51.	$C + O + M = CO + M$	1.0 (-32)	35
52.	$CO^+ + O_2 = CO + O_2^+$	2.0 (-10)	32
53.	$CO^+ + O = CO + O^\ddagger$	1.4 (-10)	33
54.	$C_2O_2^+ + O_2 = CO + CO + O_2^+$	2.0 (-10)	est.
55.	$O^\ddagger + CO_2 = O_2^+ + CO$	1.1 (-9)	33
56.	$CO^* + O_2 = CO + O_2^*$	2.0 (-10)	23
57.	$O^* + CO = O + CO^\dagger$	1.7 (-11)	36
58.	$O^* + CO = O + CO$	5.6 (-11)	36
59.	$O + CO^\dagger = O + CO$	5.9 (-15)	37
60.	$O_2^- + O = O_3 + e$	5.0 (-10)	32

TABLE 2. (continued)

No.	Reactions	k	Ref.
61.	$O_2^- + O = O_2 + O^-$	3.3 (-10)	33
62.	$O_2^- + O_2^+ = O_2 + O_2$	4.2 (-7)	33
63.	$O_2^- + O_2 = O_2 + O_2 + e$	2.0 (-18)	33
64.	$O_2^- + O_3 = O_2 + O_3^-$	4.0 (-10)	33
65.	$O_2^- + O_2^* = O_2 + O_2 + e$	2.0 (-10)	33
66.	$O^- + O_3 = O + O_3^-$	1.0 (-9)	33
67.	$O_2^+ + O_3^- = O_3 + O + O$	1.0 (-7)	38
68.	$O_2^+ + O_3^- = O_3 + O_2$	2.0 (-7)	38
69.	$O_3^- + O = O_2^- + O_2$	1.0 (-10)	38
70.	$O_3^- + O = O_2 + O_2 + e$	1.0 (-13)	38
71.	$O_2^+ + O_2 + O_2 = O_4^+ + O_2$	2.8 (-30)	33
72.	$O_2^+ + O_2 + M = O_4^+ + M$	1.0 (-31)	33
73.	$O_4^+ + O_2 = O_2^+ + O_2 + O_2$	2.0 (-13)	33
74.	$O_4^+ + O = O_2^+ + O_3$	3.0 (-10)	33
75.	$CO\dagger + He = CO + He$	1.7 (-17)	39
76.	$CO\dagger = CO + h\nu$	3.4 (+1)	40
77.	$O_2\dagger + He = O_2 + He$	1.6 (-15)	41
78.	$O_4^+ + e = O_2 + O_2$	1.1 (-7)	29
79.	$O^+ + e + M = O + M$	2.0 (-27)	33

Note that 3.8 (-12) = 3.8 X 10^{-12} cc/molecule-sec. Also † refers to vibrational excitation while * refers to electronic excitation.

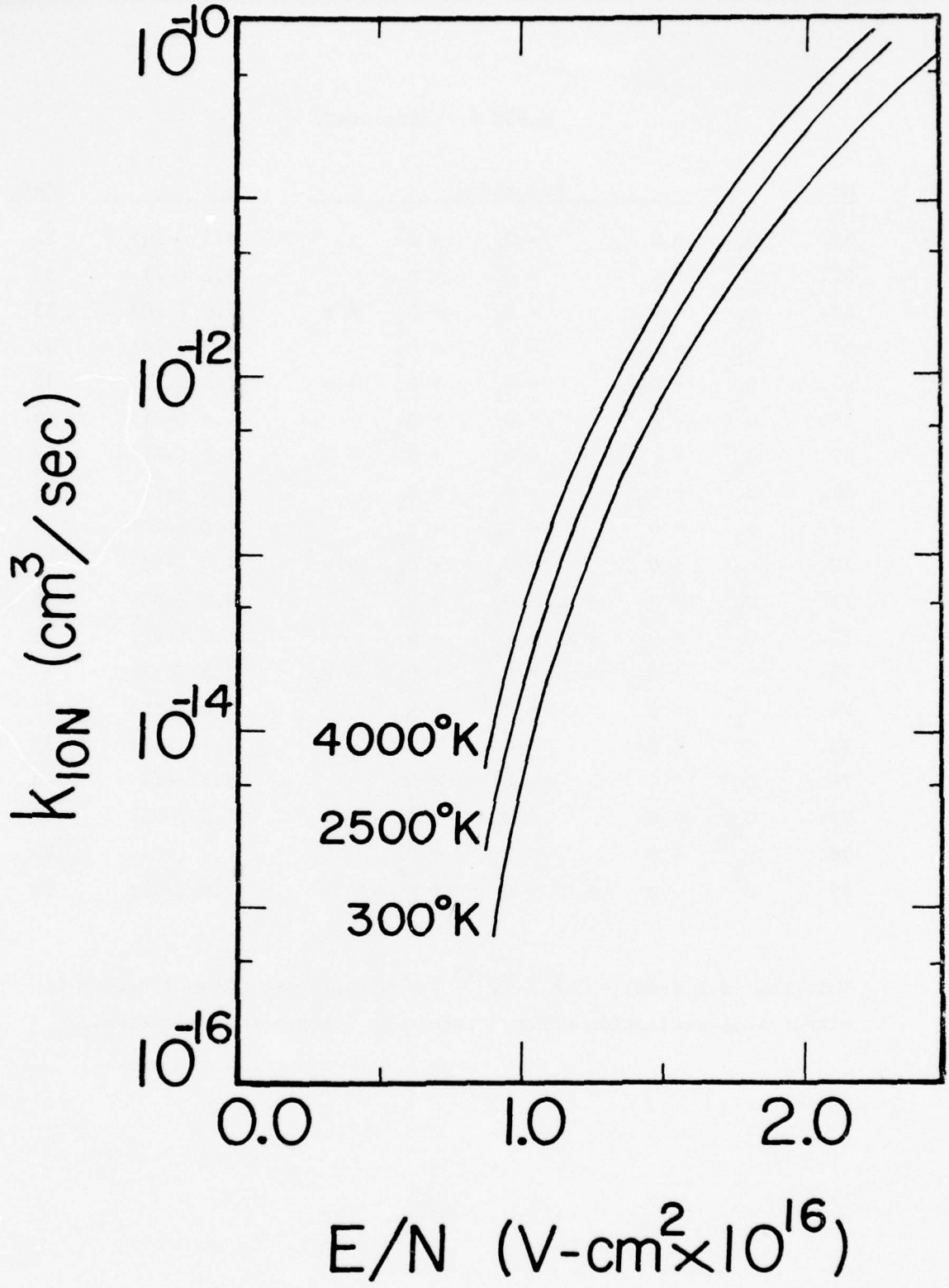


FIGURE 2: CO ionization rate coefficients for a 7% CO/93% He mixture as a function of CO vibrational temperature.

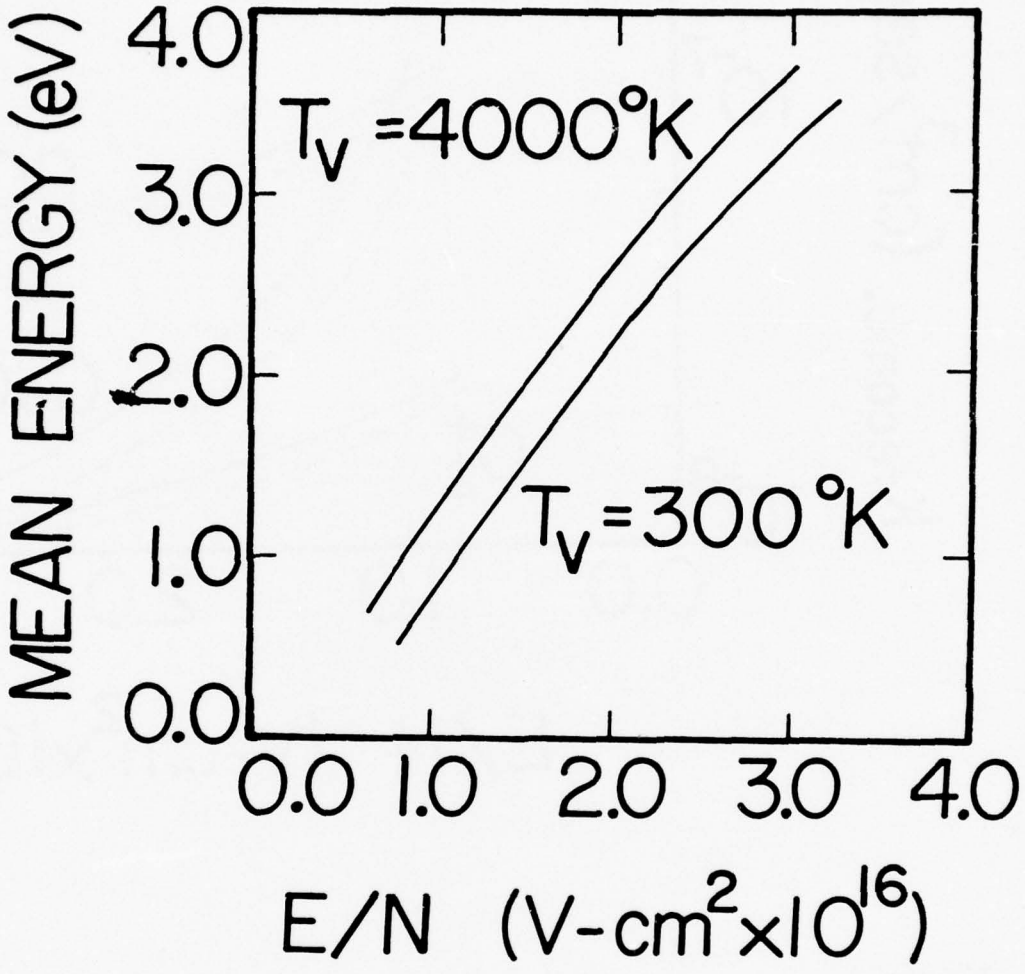


FIGURE 3: Mean electron energy as a function of E/N and CO vibrational temperature for a mixture of 7% CO/93% He.

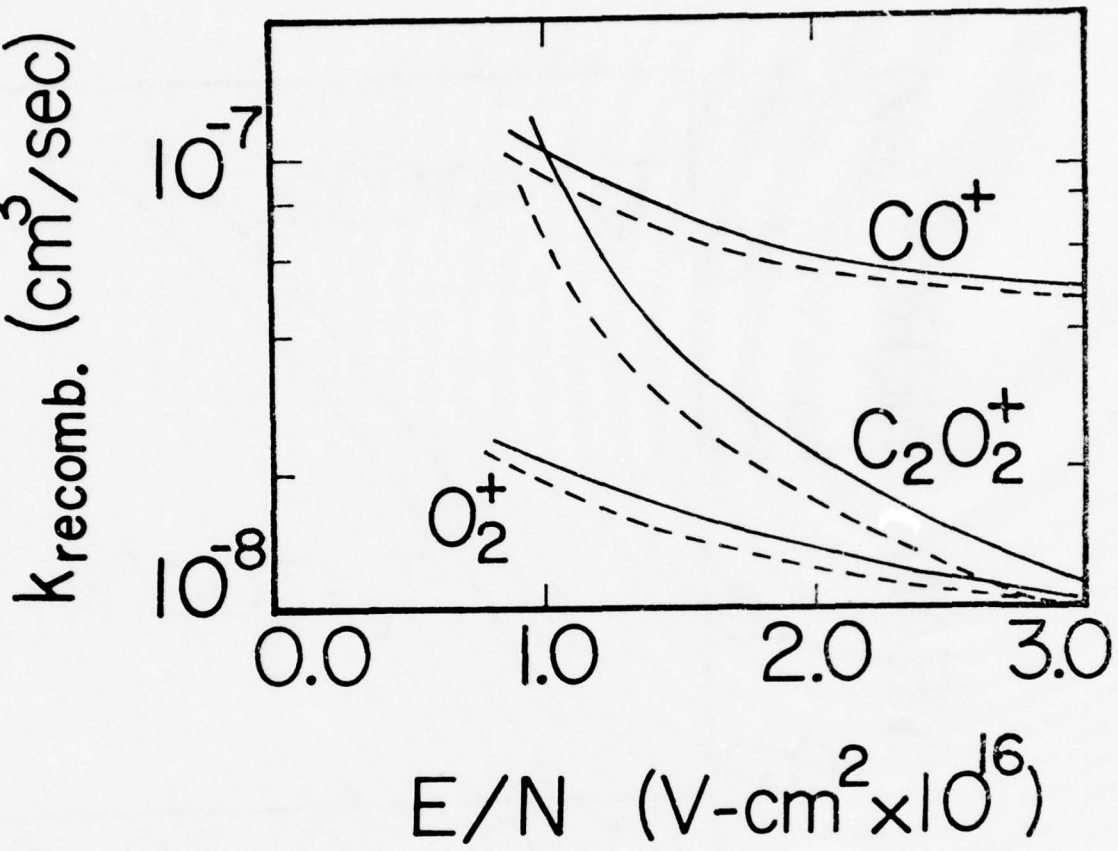


FIGURE 4: Recombination rate coefficients as a function of E/N for two CO vibrational temperatures (solid line is 300°K, dotted line is 4000°K).

CO^+, $C_2O_2^+$ and O_2^+ recombination rate coefficients. These were computed for mixtures of 1.4 torr CO, 50 m-torr O_2 and 18 torr He corresponding to the experimental conditions of Keren, et al.[18,19] The rate coefficient for recombination of $C_2O_2^+$ was obtained from center[28] who assumed that in his high pressure experiments the dominant ion was $C_2O_2^+$ or a higher order polymer ion.

The results of the calculation of the time evolution of chemical species in a CO-O_2-He discharge are displayed in Figures 5 through 8 . In these calculations, the electron density was taken to be 5×10^9 cm^{-3} initially, with a gas mixture of 1.4 torr CO, 50μ O_2 and 18 torr He and E/N equal to 1.05×10^{-16} $V\text{-}cm^2$. The initial CO vibrational temperature was chosen to be 1000°K and as it increased the electron impact rate coefficients were recomputed at T_{vib} = 1500°, 2000°, 2400°, etc. The species CO, O_2, O, O_2^* and He were included in the calculation of the electron energy distribution function, but the presence of oxygen in small concentrations has little effect upon the shape of the distribution function, even in the high energy tail.

The above calculations show that O_2^+ becomes the dominant ion in CO lasers containing O_2 due to charge transfer reactions and that, as a consequence of recombination kinetics, it is responsible for the lowering of the E/N

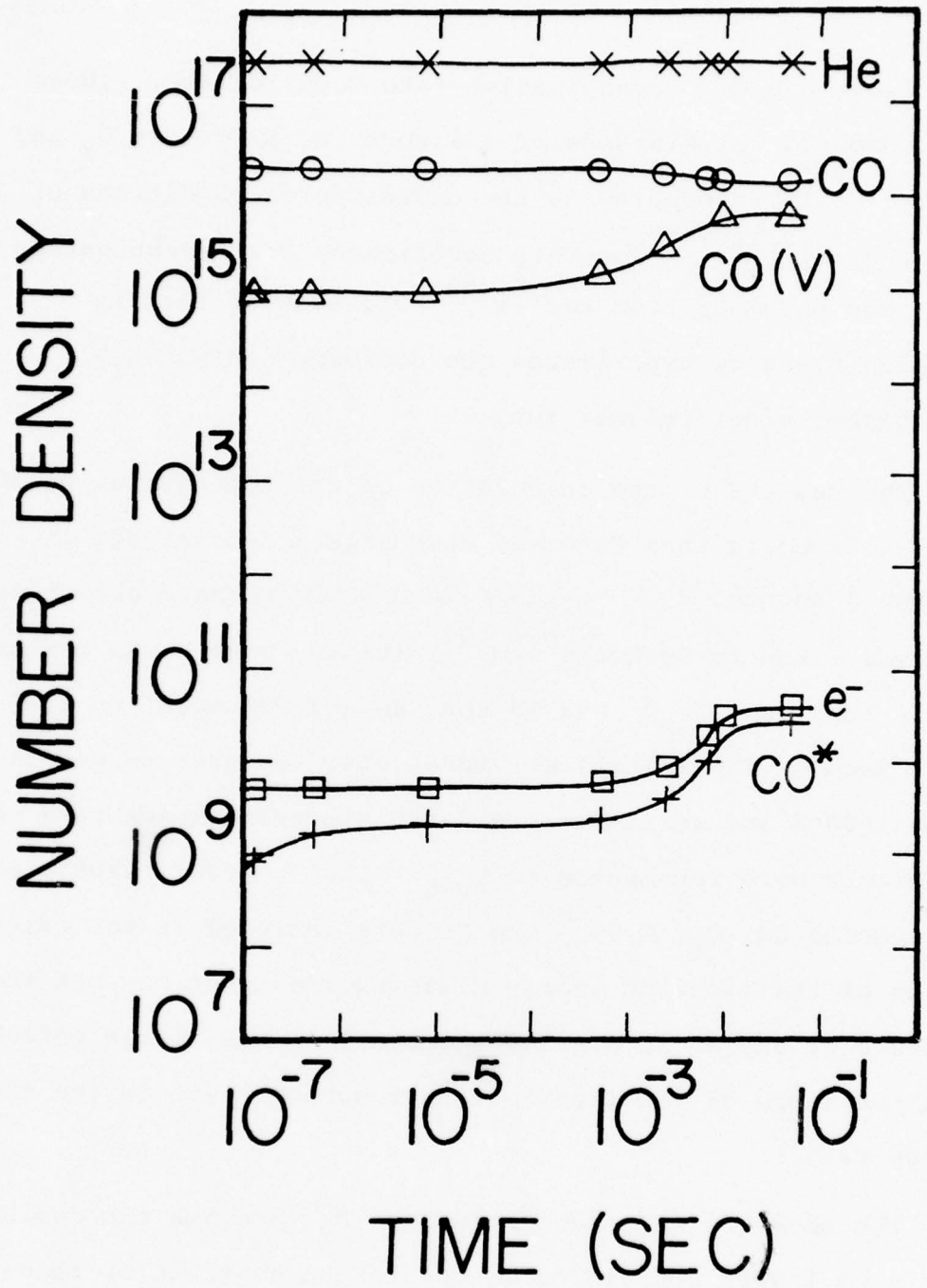


FIGURE 5: $CO/O_2/He$ kinetics at 300°K for a mixture ratio .072/.0026/.9254 at 19.5 torr.

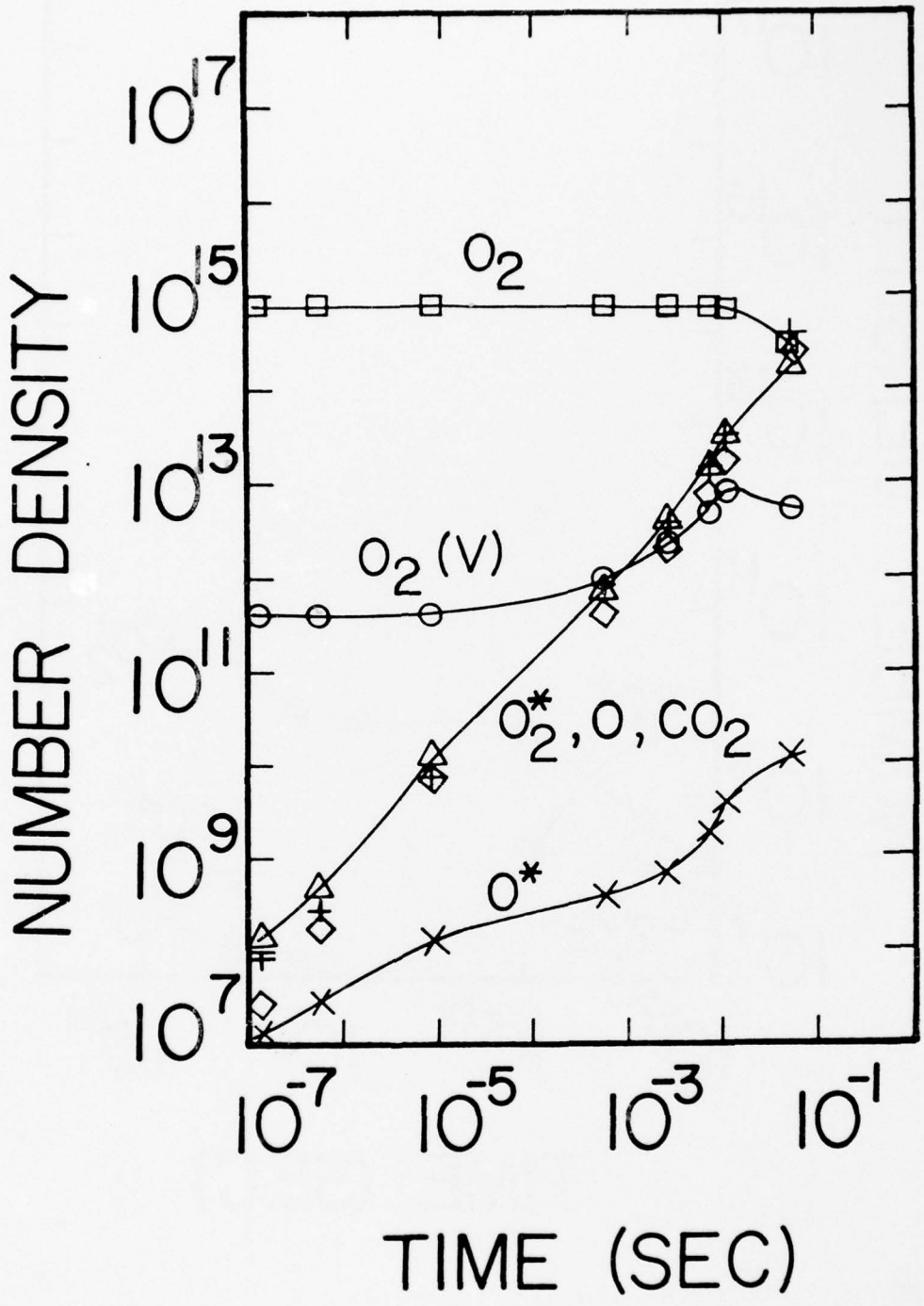


FIGURE 6 : $CO/O_2/He$ kinetics (cont'd).

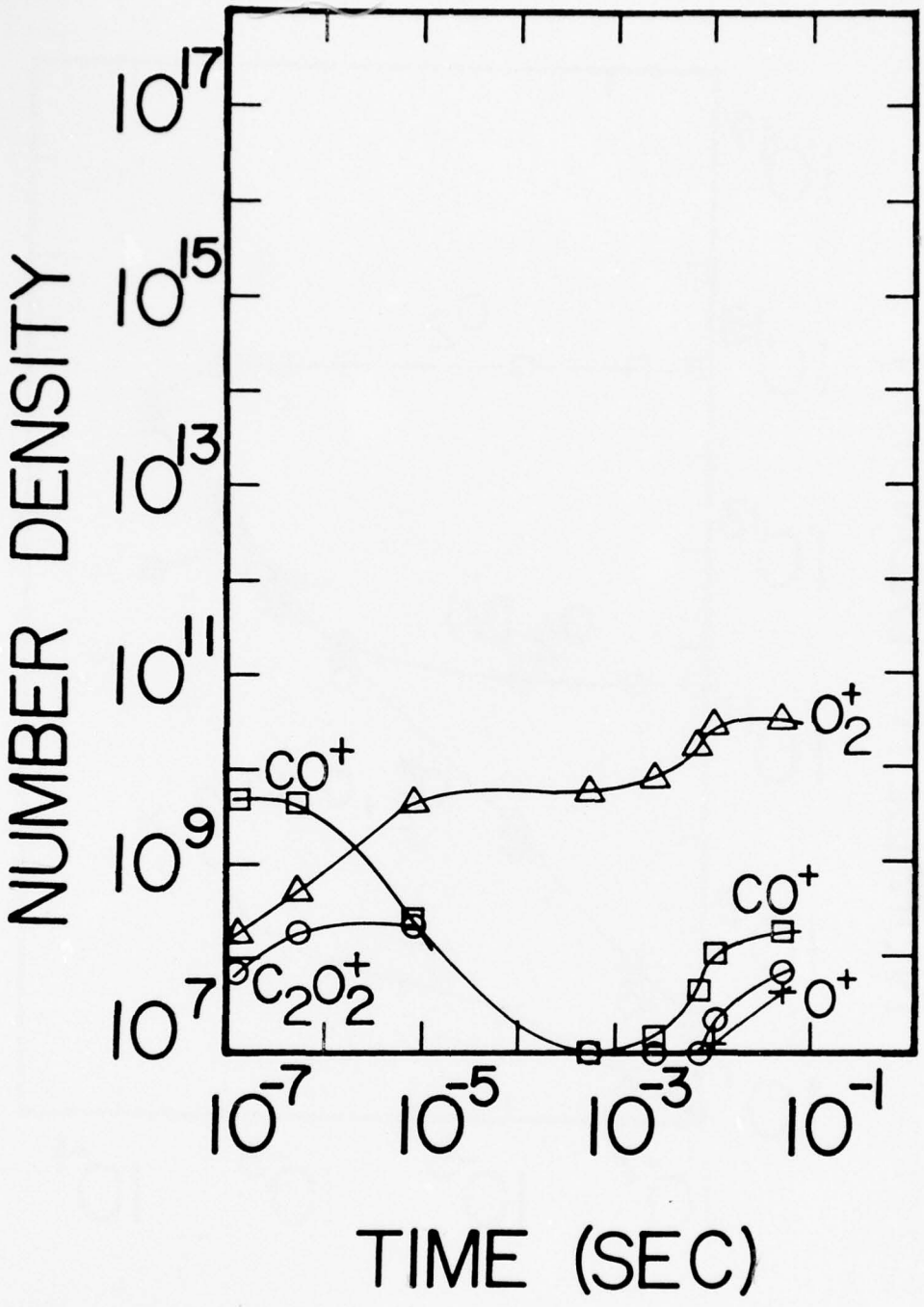


FIGURE 7: $CO/O_2/He$ kinetics (cont'd).

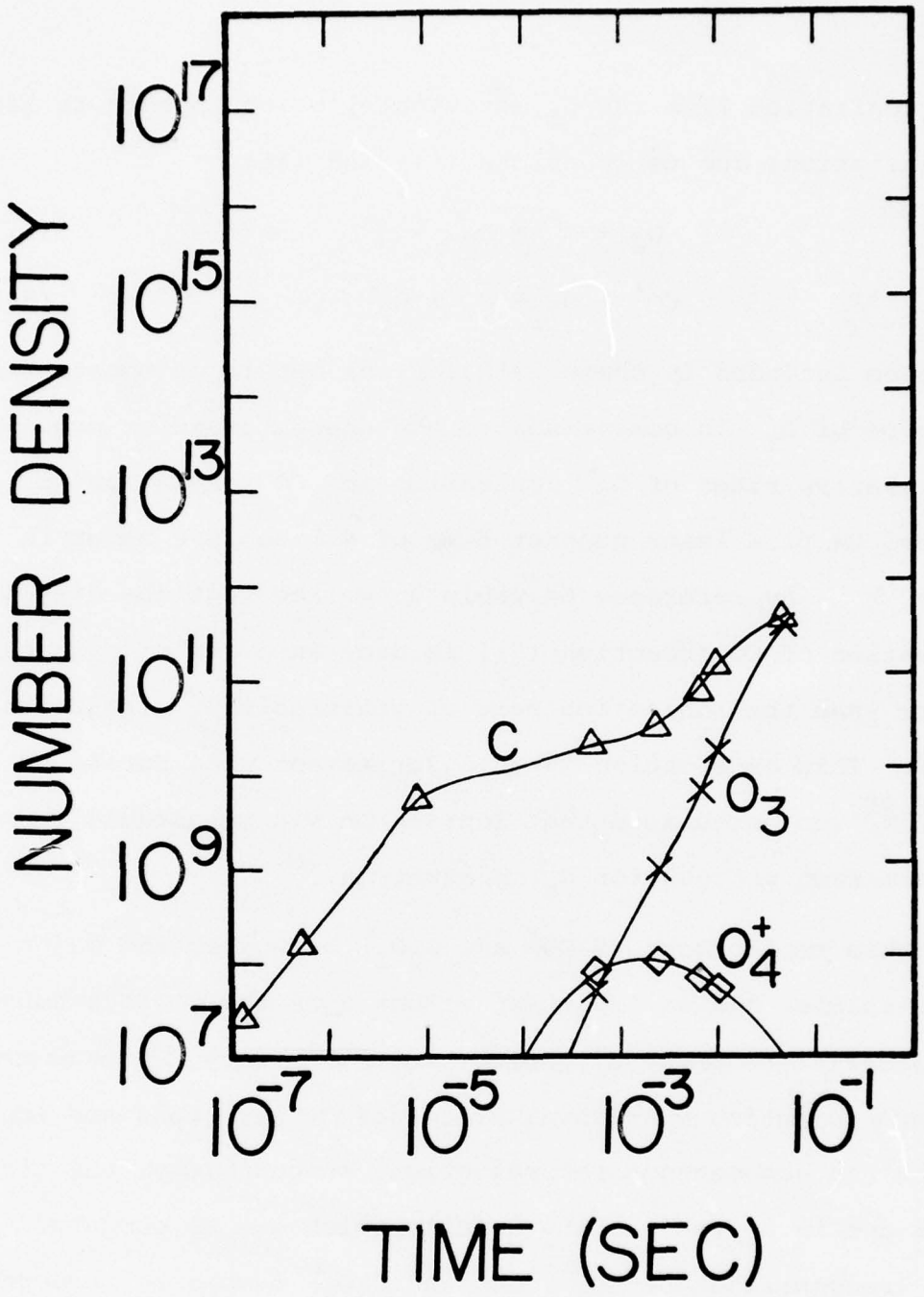


FIGURE 8: CO/O_2/He kinetics (cont'd). Note that O_2^-, O^-, C^+, O_3^- have densities below 1^7/cc.

Ionization from the O_2 metastable, which appears in large concentrations due to reactions (11) and (56),

$$O_2 + e^- \rightarrow O_2^* + e^- \qquad (11)$$

$$CO^* + O_2 \rightarrow CO + O_2^* \quad , \qquad (56)$$

has been included in these calculations but is unimportant as a source of O_2^+ in comparison to the charge transfer process. The relative rates of O_2^* ionization and CO ionization for a typical CW flow laser contact time of 0.1 sec are shown in Table 3. By reference to Table 3 we see that the direct ionization of CO [reaction (5)] is over an order of magnitude larger than the ionization rate of metastable O_2^* [reaction (20)]. This observation is in disagreement with Keren, et al[18,19] who postulated that ionization via metastable O_2 is the dominant process for O_2^+ production.

This replacement of CO^+ and $C_2O_2^+$ by O_2^+ as the major ionic species has an important effect upon the voltage-current characteristics of the discharge. For simplicity, if one assumes that the only formation and removal processes for electrons are ionization and homogeneous recombination, respectively, the electrons are in a steady state density which can be computed from (recognizing that O_2^+, CO^+ and $C_2O_2^+$ recombine through a two-body process at the pressures of interest here),

in a current regulated discharge. This is in direct opposition to the explanation advanced by Keren, et al.[18,19] This lowering of E/N allows for more efficient pumping of the CO vibrational levels as well as reduced plasma heating as a result of electronic excitation of CO followed by rapid quenching. Both factors lead to increased power output. The calcalations also demonstrate that O atoms, formed predominantly by electron impact dissociation of O_2, have an adverse effect upon laser performance when O_2 is added in large enough concentrations. This is due to relaxation of the CO laser levels by vibrational translational energy exchange in CO-O collisions. The details of these findings, and others, are presented in the following sections.

IV. RESULTS.

A. Ion Kinetics of the CO-O_2-He Discharge.

It was pointed out above that O_2^+ is found[19] to be the dominant positive ion in CO discharges containing oxygen, even when the O_2 is present in partial fractions less than 1%. The results of the calculation (Figure 7) are in agreement with this observation. The dominance of O_2^+ is due to O_2 having the lowest ionization potential of the major species in the discharge and is formed almost entirely through charge transfer reactions. $C_2O_2^+$, which is the dominant ion in CO discharges without oxygen, and CO^+ both readily charge transfer with O_2 (reaction 34).

TABLE 3. Rate constants and rates of individual reactions at t = 0.1 sec using the reactions in Table 2.

	k	Rate
1.	9.22^{-9}	5.36^{18}
2.	2.24^{-8}	5.19^{18}
3.	7.67^{-11}	4.46^{16}
4.	1.57^{-8}	1.47^{13}
5.	2.98^{-14}	1.73^{13}
6.	3.29^{-14}	1.91^{13}
7.	1.12^{-16}	6.50^{10}
8.	2.98^{-14}	6.90^{12}
9.	2.35^{-10}	1.16^{15}
10.	4.16^{-10}	3.94^{13}
11.	1.88^{-10}	9.35^{14}
12.	5.44^{-10}	2.93^{15}
13.	8.02^{-14}	3.98^{11}
14.	5.51^{-11}	2.73^{14}
15.	5.97^{-12}	2.93^{13}
16.	7.46^{-18}	3.70^{7}
17.	2.99^{-11}	1.48^{14}
18.	6.16^{-10}	1.44^{16}
19.	5.97^{-14}	1.39^{12}
20.	1.90^{-13}	1.03^{12}
21.	7.30^{-10}	4.87^{13}
22.	9.90^{-8}	3.95^{16}
23.	1.10^{-11}	4.39^{15}
24.	1.43^{-28}	8.42^{12}
25.	2.10^{-12}	4.44^{12}
26.	7.32^{-08}	3.62^{11}
27.	1.01^{-08}	1.30^{13}
28.	1.01^{-08}	1.30^{13}
29.	7.50^{-11}	1.64^{14}
30.	6.43^{-34}	1.67^{13}
31.	3.80^{-12}	3.01^{10}
32.	2.00^{-14}	6.14^{12}
33.	1.50^{-13}	9.79^{12}
34.	4.00^{-11}	2.64^{11}
35.	8.00^{-29}	3.13^{10}
36.	1.00^{-07}	1.47^{10}
37.	2.00^{-10}	5.35^{11}
38.	5.00^{-15}	2.84^{06}
39.	1.00^{-11}	1.79^{11}
40.	3.00^{-10}	1.86^{11}
41.	1.90^{-27}	8.53^{07}
42.	1.00^{-33}	1.52^{09}
43.	1.00^{-31}	7.15^{11}
44.	3.30^{-11}	4.38^{15}
45.	6.98^{-19}	2.23^{08}
46.	2.30^{-10}	7.87^{12}
47.	1.80^{-09}	5.42^{10}
48.	1.10^{-09}	1.08^{10}
49.	9.20^{-08}	8.05^{11}
50.	8.40^{-27}	2.25^{10}

TABLE 3 (cont'd)

51. 1.00^{-32}, 1.91^{12}
52. 2.00^{-10}, 1.08^{10}
53. 1.40^{-10}, 2.10^{13}
54. 2.00^{-10}, 3.61^{12}
55. 1.10^{-09}, 2.21^{13}
56. 2.00^{-10}, 6.82^{14}
57. 1.72^{-11}, 4.42^{15}
58. 5.58^{-11}, 1.43^{16}
59. 5.90^{-15}, 2.34^{16}
60. 5.00^{-10}, 1.83^{09}
61. 3.28^{-10}, 1.20^{09}
62. 4.20^{-07}, 8.42^{07}
63. 2.00^{-18}, 1.56^{00}
64. 4.00^{-10}, 1.12^{06}
65. 2.00^{-10}, 1.69^{08}
66. 1.00^{-09}, 2.05^{09}
67. 1.00^{-07}, 9.67^{07}
68. 2.00^{-07}, 1.93^{08}
69. 1.00^{-10}, 1.76^{09}
70. 1.00^{-13}, 1.76^{06}
71. 2.80^{-30}, 1.75^{09}
72. 1.00^{-31}, 1.43^{11}
73. 2.00^{-13}, 2.00^{07}
74. 3.00^{-10}, 1.41^{11}
75. 1.70^{-17}, 3.09^{16}
76. 3.36^{+01}, 2.11^{17}
77. 1.60^{-15}, 1.19^{15}
78. 1.11^{-07}, 3.05^{09}
79. 2.00^{-27}, 1.11^{09}

$$\frac{d[e^-]}{dt} = k_{ion}[e^-][CO] - k_{recomb}[e^-][ion^+] \quad .$$

If the ion and electron densities are assumed to be equal [i.e., one ion dominates and negative ions are unimportant at steady state:

$$\frac{d[e^-]}{dt} = 0 \rightarrow [e^-]_{ss} = \frac{k_{ion}}{k_{recomb}}[CO] \quad .$$

As can be seen in Figure 4, the rate coefficient for recombination of O_2^+ is substantially smaller than that of either CO^+ or $C_2O_2^+$. This results in an increased electron density when O_2^+ dominates so that, under constant current operation, the electric field must be reduced. A lower electric field increases the efficiency of electron impact excitation of the CO vibrational states as well as reducing the electron energy channeling into electronic excitation and hence heat, eventually resulting in increased power output.

As a test of this hypothesis, a simple model calculation was performed in which, given the recombination rate coefficient (as a function of electron temperature), E/N and CO vibrational temperatures were varied and the ionization rate coefficient calculated in order to achieve a chosen current density. Current density, j (amp/cm^2) is related to electron drift velocity, v_d (cm/sec) and number density, N_e (cm^{-3}) by

$$j = e v_d N_e$$

where $e = 1.6 \times 10^{-19}$ coul. and where the drift velocity v_d can be computed from the electron energy distribution function.

If a similar steady state analysis is carried out for excitation of CO(v=1) by electrons and de-excitation by superelastic collisions with electrons, which is predicted (see Table 3) to be one of the major loss processes for low vibrational levels, we find at steady state

$$\frac{[CO(v=1)]}{[CO(v=0)]} = \frac{k_{0\rightarrow 1}}{k_{1\rightarrow 0}} \quad .$$

Using these two expressions and the equation for current density we can choose an E/N and CO vibrational temperature, solve the Boltzmann equation obtaining rate coefficients, temperature and drift velocity, and calculate a current density and new vibrational temperature. This process can be repeated until the assumed and computed vibrational temperatures are equal and the desired current density has been obtained. This approach is simple, but contains the essence of the processes involved in establishing the electron density in the plasma. The greatest inaccuracy lies in the assumption concerning vibrational excitation and de-excitation of CO(v=1) since there are other important processes, such as excitation and de-excitation to and from CO(v=2,3, . . .), that affect the population of the v=1 level.

$$j = e v_d N_e$$

where $e = 1.6 \times 10^{-19}$ coul. and where the drift velocity v_d can be computed from the electron energy distribution function.

If a similar steady state analysis is carried out for excitation of CO(v=1) by electrons and de-excitation by superelastic collisions with electrons, which is predicted (see Table 3) to be one of the major loss processes for low vibrational levels, we find at steady state

$$\frac{[CO(v=1)]}{[CO(v=0)]} \simeq \frac{k_{0\to1}}{k_{1\to0}} \quad .$$

Using these two expressions and the equation for current density we can choose an E/N and CO vibrational temperature, solve the Boltzmann equation obtaining rate coefficients, temperature and drift velocity, and calculate a current density and new vibrational temperature. This process can be repeated until the assumed and computed vibrational temperatures are equal and the desired current density has been obtained. This approach is simple, but contains the essence of the processes involved in establishing the electron density in the plasma. The greatest inaccuracy lies in the assumption concerning vibrational excitation and de-excitation of CO(v=1) since there are other important processes, such as excitation and de-excitation to and from CO(v=2,3, . . .), that affect the population of the v=1 level.

Despite its defects, this calculation gives results reasonable enough to illustrate the point concerning the relationship between recombination rate, E/N and efficiency of vibrational excitation. The results are presented in Table 4. To achieve similar current densities and vibrational temperatures using the O_2^+ recombination coefficient required a 10% decrease in E/N from the value needed using the recombination coefficient for CO^+. The lowering of E/N resulted in a 34% decrease in the fraction of energy flowing into CO electronic states and a 9% increase in the fraction being channeled into v=1 alone. Thus, in contrast to Keren, et al, we have shown that O_2^+ directly affects both the E/N of the plasma and the excitation of CO vibrational energy, in agreement with the experimental observations.

B. Negative Ions in a CO Discharge.

The time development of the negative ion densities is shown in Figure 8. Although O^- is rapidly formed by dissociative attachment of CO and O_2, reactions (6) and (15), it is rapidly removed by detachment collisions with CO [reaction (21)]. This is in contrast to the chemistry of CO_2 lasers as discussed by Nighan and Wiegand[42] and by Garscadden and his collaborators,[43,44] where negative ions appear to control the stability of the discharge at low E/N. The results obtained

TABLE 4. Results of the simplified calculation of ionization-recombination processes.

	Using k_{CO^+}	Using $k_{O_2^+}$
E/N ($V\text{-}cm^2$)	1.12×10^{-16}	1.01×10^{-16}
$[e^-]$ (cm^{-3})	$4.93\times10^{+10}$	$4.99\times10^{+10}$
j (amp/cm^2)	23.4×10^{-3}	22.2×10^{-3}
$\bar{\varepsilon}$ (eV)	1.27	1.09
v_{drift} (cm/sec)	$2.97\times10^{+6}$	$2.78\times10^{+6}$
$f(CO^*)$	21.5 %	14.0 %
$f(CO_{v=1})$	18.1 %	19.8 %

here are consistent with the observations[42] that additions of CO to CO_2 lasers stabilize the discharge through electron detachment reactions with the negative ionic species.

In order for attachment to $Fe(CO)_5$ impurity to be important as pointed out by Center[28] the impurity level would have to be greater than 145 ppm. This level is substantially above the maximum level found by Center in his experiments, therefore, we expect that impurity attachment is not important to the conclusions reached in this study.

C. The Role of Atomic Oxygen in the Discharge.

As mentioned earlier in this section, at higher O_2 partial pressures the laser output power is found to decrease and the neutral temperature increase. Our calculations indicate that both of these effects are due to the formation of O atoms in the plasma. The cross sections for electron impact excitation of predissociative O_2 electronic states are large. This leads to a large production of oxygen atoms (reactions 14 and 17) and a build-up in the O atom concentration in the discharge. The calculated time development of the several neutral oxygen species is shown in Figure 6.

For very small concentrations of O_2 as an additive to CO lasers the dissociation into O atoms has little effect upon laser performance. Above some threshold O_2 concentration, the O atom density increases to a level where vibrational-translational energy transfer collisions between CO and O (reaction 59) is predicted to become the dominant de-excitation mechanism among the CO vibrational levels responsible for la-

ser action. Since it is the higher vibrational levels that dominate the laser output spectrum, the presence of O atoms will degrade the laser output. A sample of available vibrational de-excitation rate coefficients for CO(v=1) and CO(v=12) are shown in Table 5. For the low vibrational states (v=1 to v=8) superelastic collisions with electrons is the primary de-excitation process. In the absence of oxygen, radiation (reaction 76) and VT collisions with He (reaction 75) are primarily responsible for CO vibrational de-excitation. The radiative rate for CO(v=12) molecule is given by the Einstein A coefficient in Table 4. The deactivation rate for CO(v=12) by collision with He is $k_{VT}[He] = 262\ sec^{-1}$ for 18 torr of He. This is approximately the same as the radiation rate. Using a superelastic rate coefficient for the $v = 12 \rightarrow 11$ transition equal to that for the $v = 1 \rightarrow 0$ and an electron density of 10^{10} gives a de-excitation rate of $10 - 100\ sec^{-1}$. Hence radiation and He V-T exchange are likely to be the dominant de-excitation mechanisms.

However, when O atoms are present, even in small concentrations, this may strongly affect vibrational relaxation since the CO-O V-T rate coefficient for the lowest vibrational levels is more than one hundred times larger than that for CO-He.[45] If the same scaling with v is assumed for V-T relaxation by O atoms as exists for the He V-T process (a substantial underestimate based on SSH mass effect), an O atom partial pressure of only 52 m-torr would be needed for CO-O V-T to be equal to the radiation or the CO-He V-T process. Laser

TABLE 5. De-excitation of CO vibrational levels.

Process	v=1→0	v=12→11
Radiation[40] A=	$33.6\ sec^{-1}$	$239.9\ sec^{-1}$
V-T with He[39], k= ($T_{gas}=300^{o}K$)	$1.7x10^{-17}\ cm^3/sec$	$9.0x10^{-16}\ cm^3/sec$
V-T with O[37], "	$5.9x10^{-15}$ "	$\geq 2.9x10^{-13}$† "
V-T with O_2[48], "		$2.1x10^{-14}$ "
V-T with CO_2[48],"		$8.6x10^{-14}$ "
Superelastic with e^-, "	10^{-9}-10^{-8}†† "	

†The value shown is computed assuming the same scaling with v as the CO-He V-T process.

††The rate coefficient is typically in this range with its exact value depending upon the electron energy distribution function.

performance will be degraded when the contribution of the CO-O V-T rates is non-negligible in comparison to the fixed radiation and CO-He V-T rates. The scaling of vibrational rate coefficients with increasing vibrational level is, in general, uncertain. However, the collision system of $O(^3P)$ + $CO(^1\Sigma,v')$, which correlates with the triplet state of CO_2, offers the possibility of a strong "chemical" interaction through curve crossing to the $CO_2(^1\Sigma)$ state and enhanced energy transfer possibilities associated with a short lived triatomic complex.

Although the above arguments are somewhat qualitative due to a lack of reliable rate constant data information, our chemistry calculations predict substantial dissociation, larger than 20%, for time scales of the order of flow contact times in typical CO lasers. For dissociation levels of this order, O atom VT processes will substantially reduce the vibrational content of CO, leading to reduced laser output as well as increased plasma heating.

The effect of higher O_2 additions on the shape of the experimentally observed CO vibrational distribution up to $v \cong 30$ also clearly shows the emergence of a strong VT process, attributable to O atoms.[45,46]

It can be seen from the rate coefficients in Table 5 that vibrational relaxation by O_2 will be unimportant for the concentrations being discussed here. The same will be true for small concentrations of CO_2, which is formed primarily by reactions (21) and (23):

$$O^- + CO \rightarrow CO_2 + e^- \qquad (21)$$

$$CO^* + CO \rightarrow C + CO_2 \ . \qquad (23)$$

The density of CO_2 is still increasing, however (Figure 7), at the end of the calculation indicating that there may be a large buildup of this species in closed CO systems. In flowing discharges with a residence time of .1 - .5 sec this may not be a problem, but in a sealed system, CO_2 may be present in large enough concentrations to be a major source of vibrational de-excitation.

D. Additional Discussion of CO Laser Chemistry.

We propose that carbon in the CO laser is formed primarily as a product in the quenching of electronically excited CO, i.e., reaction (23). Reactions (22) and (23),

$$CO^* + CO \rightarrow CO^\dagger + CO^\dagger \qquad (22)$$

$$CO^* + CO \rightarrow C + CO_2 \quad , \qquad (23)$$

correspond to two channels for de-excitation of CO^* by CO. The total rate coefficient is known,[23] but the branching ratio is not. It has been assumed in these calculations that 10% of the CO^* + CO reactions follow the C + CO_2 branch. The C production rate is critically dependent upon this branching ratio and there is, unfortunately, no information on the branching ratio or even on the carbon concentrations found in CO discharges. The carbon is readily removed by reaction (44)

$$C + O_2 \rightarrow CO^\dagger + O^* \qquad (44)$$

with O_2. This is a satisfactory explanation of the observation that the addition of O_2 to a CO discharge reduces or eliminates carbon deposition in the system. The products of this reaction have been assumed to be $CO^\dagger$ and $O(^1D)$ as these are spin allowed and energetically accessible.

Finally, mention should be made of the possible role of $O(^1D)$ in the discharge. It is rapidly formed by reactions (17), (18) and (28):

$$O_2 + e^- \rightarrow O + O^* + e^- \quad (17)$$

$$O + e^- \rightarrow O^* + e^- \quad (18)$$

$$O_2^+ + e^- \rightarrow O + O^* \quad (28)$$

and, perhaps, (44) as discussed above. The O^* is then rapidly removed in reactions (57) and (58):

$$O^* + CO \rightarrow O + CO^\dagger \quad (57)$$

$$O^* + CO \rightarrow O + CO \ . \quad (58)$$

Although O^* has little effect upon the chemistry of the system it may, in this way, be an important source for heating the gas.

Using the reaction rates for both $O(^1D)$ quenching into translational energy (reaction 58) and relaxation of $CO^\dagger$ into translational energy (reaction 59) as given in Table 3, the total energy flux from these reactions is sufficient to explain the observed[17] gas temperature increase with increasing O_2 pressure beyond the optimum pressure for laser output.

V. HETEROGENEOUS VERSUS HOMOGENEOUS ELECTRON LOSS PROCESSES

In low pressure, small diameter laser discharges, ambipolar diffusion can dominate the electron loss mechanism. Here we consider the competition between homogeneous recombination and ambipolar diffusion in controlling the electron density in a CO laser system.

In order to estimate the relative contribution to the electron loss rate, the time scale associated with diffusion and recombination must be estimated. The time scale for diffusion loss is found from a solution to the radial diffusion equation as

$$\tau_{diff} = \frac{e}{kT_e} \quad \frac{\Lambda^2}{\mu_+}$$

where μ_+ is the ion mobility, T_e is the mean electron temperature and Λ is the characteristic diffusion length ($\Lambda \geq R/2.4$ where R is the tube radius). For a 20 torr, 300°K plasma in which CO^+ is the dominant ion (taking R = 1.5 cm and T_e = 0.9 eV)[47]

$$\tau_{diff}^{CO^+} = 5.1^{-4} \text{ sec.}$$

The ambipolar diffusion time for O_2^+ as the dominant ion is only slightly slower than that of CO^+ $\left(\tau_{diff}^{O_2^+} = 4.7^{-4} \text{ sec}\right)$ under the same conditions.[47] Evidence suggests that the diffusion of ion clusters in the case of $C_2O_2^+$ is not substantially different from the parent ion.

The time scale for homogeneous recombination can be estimated from the rate of the recombination reactions, (26) in the case of $C_2O_2^+$ and (27) + (28) in the case of O_2^+. Thus,

$$\tau_{recomb}^{C_2O_2^+} = 4.6^{-4} \text{ sec}$$

and

$$\tau_{recomb}^{O_2^+} = 1.7^{-3} \text{ sec.}$$

These estimates show that the ambipolar loss time scale and the homogeneous recombination time scale are of the same order. At higher pressures and lower temperature operation the homogeneous recombination process will dominate and the calculations presented above on the influence of oxygen in the electron density will more quantitatively apply. Under the conditions of the calculations presented in this study, the quantitative predictions will be reduced, but the substitution of O_2^+ as the dominant ion will still clearly reduce the rate of electron loss and produce a corresponding increase in electron density at constant E/N.

VI. SUMMARY AND CONCLUSION.

We have attempted to demonstrate a consistant interpretation to the effects of small amounts of molecular O_2 in a low pressure CW CO/He laser system. The observation that very small amounts of O_2 lead to a reduction in E/N, a reduction in plasma temperature and an increase in output power we attribute to the emergence of O_2^+ as the dominant positive ion. Since O_2^+ recombines more slowly than CO^+ or its polymers at the E/N of interest, the same current can be maintained by a lower E/N. The reduction in E/N results in a more favorable fraction of the electron energy into vibration with a corresponding decrease of electron energy into CO electronic states. The thermal energy produced by electronic quenching (E-V/T) is reduced and the plasma cools. The simultaneous improved vibrational excitation and reduced plasma temperature leads to improved laser energy output.

At higher O_2 additions, the O atoms generated primarily by predissociation of O_2 lead to direct deactivation of the upper vibrational levels of CO responsible for lasing through

VT processes as well as increased plasma temperatures through $O(^1D)$ formation by electron impact followed by quenching by CO through E-V/T processes. These two O atom effects lead to a degradation of laser output.

The dynamics of carbon formation and loss is proposed to occur through electronically excited CO but is not found to be important in the laser dynamics except to influence the laser lifetime. This latter effect occurs when the carbon deposits increase cavity losses such that lasing ceases.

The importance of plasma chemistry processes involving minor constituents attests to the complexity of molecular discharge sustained lasers. The dominance of recombination kinetics as opposed to ionization processes suggests that other additives might enhance laser output in ways previously unappreciated.

Lastly, we would like to remark on the role of superelastic processes in the CO laser system. It is clear that superelastic feed-back from the vibrationally excited CO is critical in determining observed ionization rates, and hence electron densities. We would like to suggest that superelastic processes are also responsible for the normal negative E vs. I characteristics measured in low temperature CO lasers and for the deviation to a positive E vs. I characteristic observed under higher temperature operation. We sug-

gest that without O_2, the E/N of the discharge is high but that at liquid N_2 cooling the CO vibrational modes are still sufficiently excited that the superelastic feed-back determines the ionization rate and electron density. As the E/N is reduced, a more favorable vibrational excitation by electrons is produced coincident with a reduction in plasma temperature. The subsequent increase in vibrational excitation leads to increased superelastic feed-back, greater ionization and an increased electron density, i.e., current. This behavior demonstrates a negative E vs. I characteristic.

Under very high plasma temperatures such as maintained by Keren, et al, the superelastic contribution is minimal. Therefore, the ionization is determined by the high energy tail of the electron distribution as provided by the E/N. When the E/N is reduced the high energy tail is depressed leading to reduced ionization rates and lower electron densities, i.e., a reduction in current. This behavior is characterized by a positive E vs. I characteristic.

It is clear from this suggestion that low temperature operation or the presence of additives would give negative E vs. I behavior in agreement with observation. Since the only positive E vs. I characteristic has been reported under high temperature operation, we believe this explanation is consistent with available experimental observation.

REFERENCES

1. R. E. Hake and A. V. Phelps, Phys. Rev. 158, 70 (1967).
2. H. Ehrhardt, L. Langhans, E. Liner and H. S. Taylor, Phys. Rev. 173, 222 (1968).
3. D. Rapp and D. D. Briglia, J. Chem. Phys. 43, 1480 (1965).
4. L. J. Kieffer, JILA Report No. 13, September (1973).
5. S. Trajmar, D. C. Cartwright, W. Williams, Phys. Rev. A4, 1482, (1971).
6. C. E. Watson, et al, J. Geophys. Res. 72, 3961 (1967).
7. L. D. Thomas and R. K. Nesbet, Phys. Rev. A11, 170 (1975).
8. J. M. Ajello, J. Chem. Phys. 55, 3158 (1971).
9. S. Chung and C. C. Lin, Phys. Rev. A8, 2463 (1973).
10. T. Sawada, D. L. Sellin and A.E.S. Green, J. Geophys. Res. 77, 4819 (1972).
11. H. F. Schaefer III and W. H. Miller, J. Chem. Phys. 55, 1107 (1971). This transition is thought to go to the $c^1\Sigma_u^-$ state rather than the $A^3\Sigma_u^+$ state by S. Trajmar, W. Williams and A. Kupperman, J. Chem. Phys. 56, 3759 (1972).
12. P. H. Krupenie, J. Phys. Chem. Ref. Data. 1, 423 (1972).
13. P. D. Burrow, J. Chem. Phys. 59, 4922 (1973).
14. W. L. Nighan, Phys. Rev. A2, 1989 (1970).
15. S. Yarema, M.S. Thesis, Department of Electrical Engineerig, Wayne State University, June (1974).
16. M. L. Bhaumik, W. B. Lacina and M. M. Mann, IEEE J.Q.E. 8, 150 (1972).
17. T. S. Hartwick and J. Walder, IEEE J.Q.E. 8, 455 (1972).
18. H. Keren, P. Avivi and F. Dothan, IEEE J.Q.E. 11, 590 (1975).
19. H. Keren, P. Avivi and F. Dothan, IEEE J.Q.E. 12, 58 (1976).

20. W. Lowell Mrogan and Edward R. Fisher, "Calculations on the Electron Energy Distribution in a Molecular Laser Plasma," RIES Report 74-56, Wayne State University, August (1974).

21. T. Keneshea, Air Force Cambridge Research Laboratory, Report No. AFCRL-67-0221, Environmental PaPer No. 263 (1967).

22. D. A. Parkes, Trans. Faraday Soc. 68, 627 (1972).

23. G. W. Taylor and D. W. Setser, J. Chem. Phys. 58, 4040 (1973).

24. J. J. Leventhal and L. Friedman, J. Chem. Phys. 46, 997 (1967).

25. M. Saporoschenko, J. Chem. Phys. 49, 768 (1968).

26. S. L. Chang and J. L. Franklin, J. Chem. Phys. 54, 1487 (1971).

27. R. L. Horton, J. L. Franklin and B. Masseo, J. Chem. Phys. 62, 1739 (1975).

28. R. E. Center, J. Appl. Phys. 44, 3538 (1973).

29. J. M. Bardsley and M. A. Biondi, "Dissociative Recombination," in Advances in Atomic and Molecular Physics, ed. D. R. Bates, Vol. 6 (Academic Press, New York, 1970).

30. R. J. Donovan and D. Hussain, Chemical Reviews 70. 489 (1970).

31. K. Schofield, Planet. Space Sci. 15, 643 (1967).

32. E. W. McDaniel, et al, Ion-Molecule Reactions (Wiley-Inter-Science, New York, 1970).

33. M. H. Bortner, R. H. Kummler and T. Baurer, "Summary of Suggested Rate Constants," Defense Nuclear Agency Reaction Rate Handbook, Ch. 24, DNA 1948H (Revision No. 5, September 1973).

34. E. W. McDaniel, Collision Phenomena in Ionized Gases (Wiley, New York, 1964).

35. M. B. McElroy and J. C. McConnell, J. Geophys. Res. 76, 6674 (1971).

36. R. G. Shortridge and M. C. Lin, to be published in J. Chem. Phys.

37. R. E. Center, Proc. Ninth Int. Shock Tube Symposium, ed. D. Bershader and W. Griffith (Stanford University Press, Stanford, Calif. 1973).

38. F. E. Niles, J. Chem. Phys. 52, 408 (1970).

39. M. R. Verter and H. Rabitz, J. Chem. Phys. 64, 2939 (1976).

40. G. Abraham and E. R. Fisher, J. Appl. Phys. 43, 4621 (1972).

41. R. C. Millikan and D. R. White, J. Chem. Phys. 39, 3209 (1963).

42. W. L. Nighan and W. J. Wiegand, Phys. Rev. A10, 922 (1974).

43. J. F. Prince and A. Garscadden, Appl. Phys. Lett. 27, 13 (1975).

44. P. Bletzinger, et al, IEEE J.Q.E. 11, 317 (1975).

45. E. R. Fisher and A. J. Lightman, manuscript in preparation (1977).

46. A. J. Lightman and E. R. Fisher, Appl. Phys. Lett. 29, 593 (1976).

47. W. Lindinger and D. L. Albritton, J. Chem. Phys. 62, 3517 (1975).

48. G. Hancock and I.W.M. Smith, Appl, Optics 10, 1827 (1971).

Appendix II

Abstracts of papers presented at the 5th Conference on Chemical and Molecular Lasers

St. Louis, Mo. April 18-20, 1977

(1)*An Analytical Theory of Vibrational Relaxation for Anharmonic Oscillators Under Strongly Pumped Conditions, S.H.Lam,Princeton University.

(2) Measurements of CO Vibrational Distributions in Mixtures with N_2, O_2, Ar and He, A.J.Lightman and E.R.Fisher, RIES, Wayne State University.

(3) Comparison of Experimental and Theoretical Vibrational Population Distributions in Electric Discharge CO-He Mixtures, E.R.Fisher, RIES, Wayne State University, H.Rabitz and S.H.Lam, Princeton University.

(4) Plasma Chemistry and Energy Transfer Processes in $CO-O_2$-He and $CO-N_2$-He Mixtures, E.R.Fisher and G. Abraham, RIES, Wayne State University.

*Professor Lam's first paper was supported by AFOSR (F44620-73-0059). It is included here since it forms, together with the following 3 papers, a fully consistent interpretation of the dynamics of high lying vibrational states in CO.

An Analytical Theory of Vibrational Relaxation for Anharmonic Oscillators Under Strongly Pumped Conditions. S. H. LAM, Princeton U.* -- An analytical theory for the quasi-steady vibrational population distribution, N_i, of a diatomic gas under strong vibrational excitation will be presented, showing explicitly the dependence of N_i on the relevant VV and VT kinetic rates, temperature, anharmonicity of the energy levels, and the strength of the external pumping. It is shown that from the large collections of VV and VT rates needed for the master kinetic equations, two parameters and two functions suitably extracted are the only important information required. The location of the Treanor-Plateau and the Plateau-Boltzmann boundaries, the ground-level vibrational temperature, the amount of vibrational energy dissipated by VV and VT collisions (in quasi-steady situations) and the magnitude of the Plateau are obtained. These explicit analytical results can be used to deduce quantitative information from experimental N_i measurements on the kinetic rates, particularly the VT rates at high quantum numbers.

*This research was supported by AFOSR (F44620-73-0059).

Abstract Submitted to the

5th Conference on Chemical and Molecular Lasers

April 18, 19, 20, 1977

Measurements of CO Vibrational Distributions in Mixtures with N_2, O_2, Ar and He.* A.J. LIGHTMAN and E.R. FISHER, RIES, Wayne State U.--The first and second overtone infrared emission from a discharge sustained CO laser plasma(1) in mixtures with N_2, O_2, Ar and He has been measured. A 2.5cm diameter fast flow laser tube was liquid nitrogen cooled and was operated with CO partial pressures from 0.5 to 1.5 torr total pressures from 4 to 16 torr and currents from 5 to 15 ma. Least squares analysis of the data yielded the rotational temperature and the relative vibrational populations in CO from v = 2 to v = 30. Detailed model calculations on the CO-He system have yielded energy transfer scaling relationships to high vibrational states.(2) Under constant partial pressures and for varying currents from 5 to 15 ma in CO-He, a clear radial variation in the electron density is indicated. Measurements in CO-N_2-He mixtures show the enhancement in the distribution due to N_2-CO VV pumping. Measurements on CO-N_2-AR mixtures show higher rotational temperatures than with He and give insight into the effect of mass on the scaling of VT processes. Detailed measurements on increasing O_2 additions to both CO-He and CO-N_2-He mixtures show enhanced distributions for small O_2 additions and clear VT effects in the upper states for higher O_2 additions.

*partially supported by DARPA through ONR-Boston.

(1)A.J. Lightman and E.R. Fisher, Appl. Phys. Lett. 29, 593 (1976).

(2)E.R. Fisher, H. Rabitz and S.H. Lam, following paper.

(3)W.L. Morgan and E.R. Fisher, manuscript in preparation.

Submitted by

Edward R. Fisher

Edward R. Fisher
RIES
220 Engineering Bldg.
Wayne State University
Detroit, Mich. 48202

Comparison of Experimental and Theoretical Vibrational Population Distributions in Electric Discharge CO-He Mixtures.* E. R. FISHER, Wayne State U., H. RABITZ, and S. H. LAM, Princeton U. Theoretical predictions of vibrational population distributions (N_i) have always been hampered by the uncertainties of the relevant kinetic rates in the master kinetic equations. The present paper compares detailed experimental measurements of N_i in CO-He mixtures ($T° \cong 140°K$, $0 \leq i < 30$) with theoretical calculations using various rate models. These calculations are shown to be particularly sensitive to the VT rates assumed. Using the recent theoretical rates of Verter and Rabitz, reasonable agreements between theory and experiments are obtained. By slightly adjusting the Verter-Rabitz rates, excellent agreements have been obtained. The Verter-Rabitz rates have a distinctly slower quantum number dependence than conventionally assumed (extrapolations using SSH) at this temperature, and the results of the present study give strong support to this distinctive feature. The effects of VV rate models are also studied and will be discussed.

*This research was supported partially by DARPA through ONR-Boston and partially by AFOSR.

Abstract Submitted to the

5th Conference on Chemical and Molecular Lasers

April 18, 19, 20, 1977

Plasma Chemistry and Energy Transfer Processes in $CO-O_2-He$ and $CO-N_2-He$ Mixtures. E.R. FISHER and G. ABRAHAM, RIES, Wayne State U.--Experimental evidence as well as past model calculations have demonstrated the important coupling between the plasma ion chemistry, neutral chemical reactions and energy transfer processes in affecting the output and efficiency of discharge sustained CO molecular lasers. When a small amount of O_2 is added to a CO-He mixture the output power is known to be increased while larger additions cause the output to degrade. In past work(1) we have used a coupled laser model incorporating a non-Boltzmann electron energy code, a transient ion and neutral chemistry code, and a detailed energy transfer model to explain these and other O_2 observations. The laser enhancement is a result of the recombination dynamics of O_2^+ compared to CO^+ (or $C_2O_2^+$) while the output degradation is a result of O-atom VT relaxation. The plasma chemistry and energy transfer codes used above have been extended to include N_2 and N containing species. In particular, relatively high concentrations of CN, and the electronically excited $A^2\pi$ and $B^2\Sigma$ states of CN, have been observed in $CO-N_2-He$ mixtures. A decrease in laser power output has been shown to be correlated to the presence of CN species in the plasma. The chemistry of CN in the CO laser will be discussed using our detailed numerical model together with experimental evidence from our laboratories and elsewhere. As a prelude to the N_2 chemistry model, the earlier results on O_2 additions will be summarized.

(1)W.L. Morgan and E.R. Fisher, manuscript in preparation.

Submitted by

Edward R. Fisher

Edward R. Fisher
RIES
220 Engineering Bldg.
Wayne State University
Detroit, Mich. 48202

Appendix III

"CO Vibrational Distributions to High Levels
in Low Pressure CO/He Mixtures"

Allan J. Lightman and Edward R. Fisher

CO Vibrational Distributions to High Levels in Low Pressure CO/He Mixtures*

Allan J. Lightman**
Department of Electrical and Computer Engineering

and

Edward R. Fisher**
Department of Chemical Engineering
Wayne State University
Detroit, Michigan 48202

April 1977

*This work was partially supported by DARPA through ONR-Boston on Contract No. N00014-75-C-0284.

**Members Research Institute for Engineering Sciences

Acknowledgment

The authors thank Mr. Sung Won Kim and Mr. Michael Klicek for help in the experiments and Mr. Soon Lim for fitting the measured spectra. Also appreciation is expressed to Professors S.H. Lam and H. Rabitz of Princeton University for discussions on the experiments and conclusions.

Abstract

Experimental measurement of the 1st and 2nd overtone spontaneous emissions spectrum in a low pressure CO/He plasma has enabled determination of the vibrational distribution up to v = 30. The variation in the CO distribution as a function of CO and He partial pressure and plasma current has been correlated by a detailed model of the steady state energy transfer dynamics. The agreement between calculated and measured distributions has generated a consistent set of rate coefficients for CO/He mixtures for a temperature around 150 K.

Introduction

The CO laser, due to its high efficiency, has undergone detailed investigation since its first demonstrated performance by Patel [1]. A great deal of effort has gone into understanding and modifying the operating conditions to both improve efficiency and enhance certain spectral operating regions. These effects are often achieved by altering the plasma environment in which the excitation process is produced and by altering the chemical kinetic processes affecting excitation. In order to aid our understanding and analysis we have underway a detailed study of plasma effects which are observed by analyzing the overtone spectra from a flowing, continuous-electric-discharge, CO laser system.

The 1st and 2nd overtone spectra are measured using the end-light spontaneous emission from the discharge tube. In this configuration we have been able to observe output corresponding up to the 35th vibrational level in CO with substantial signal-to-noise [2]. We are not yet limited in observation by any physical considerations. Using this overtone spectra we have calculated the CO vibrational distribution up to $V \lesssim 30$ and thereby determined directly the effects on the vibrational distribution resulting from changes in the plasma environment, either electrical and/or chemical. The experiments analyzed and reported in this paper are restricted to the binary mixture CO/He. We have varied the relative partial pressures of CO and He in a systematic fashion and have found a set of energy transfer rate coefficients which are both consistent with available rate data and will model all observations successfully. This paper reports these rate coefficients for the CO/He system, the measurement technique used to generate the CO vibrational distributions, and the analytical laser model developed to correlate the observed distributions. Measurements coordinated with analytical modeling are underway on other relevant mixtures involving CO, e.g. $CO/N_2/He$, $CO/O_2/He$ and CO/Ar. The results of these studies will be detailed in forthcoming papers.

II. Measurements

The overtone spectra in CO were observed using the spontaneous end-light emission from a liquid-nitrogen cooled electric-discharge laser tube, with all laser action blocked. The end light was analyzed by a quarter-meter low resolution scanning spectrometer with a cooled PbS detector. The data was simultaneously displayed on an X-Y plotter and recorded on an FM recorder for computer analysis.

The medium was checked for optical thinness by placing a mirror at the end of the discharge tube to reflect the radiation back to the detector. It was observed that the increase in intensity was a constant proportion of the signal indicating no significant self-absorption.

One of the features of this tube, which later played an important role in the analysis, was a teflon collar placed over the edge of the anode to block out plasma contact at the edge. This collar insured that the discharge connected to the large area of the inner surface of the concentric ring electrode as shown in Figure 1.

The gases were premixed and pumped into the discharge volume. The composition could be accurately controlled using a calibrated rotometer for each constituent. Starting from the nominal mixture that gave optimal laser performance, the 1st and 2nd overtone CO spectra were measured in mixtures for which $0.5 \leq P_{CO} \leq 1.5$ and $4 \leq P_{He} \leq 16$ torr. For each run the voltage across the positive column was monitored so that, together with the composition and total pressure data, the plasma could be characterized.

The intensity versus wavelength data was transferred to a high-speed digital computer and analyzed. As a first step, the spectrum was corrected for system response functions by using the recorded spectrum of a calibrated "grey-body" viewed from behind the end of the laser tube. The data was simulated using standard infrared vibrational transition profiles, convoluted

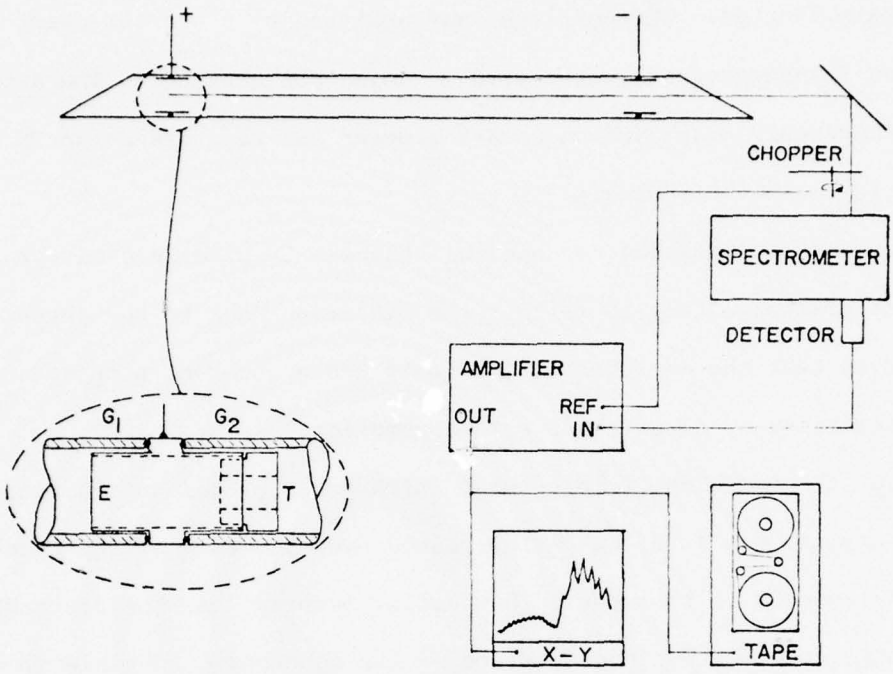


Figure 1. Experimental arrangement for spontaneous end-light measurement showing expanded electrode structure (E=electrode, T=teflon collar, and G_1, G_2 = pyrex plasma tube).

with the spectrometer window profile and then fitted by a least-squares adjustment technique to the observations. As a result of the fit we obtain the relative population distribution in CO. Because of the overlap of the high v states of the 2nd overtone with the low v states of the 1st overtone spectra the least-squares fit had to be done iteratively.

A representative spectra and the resulting fit are shown in Figure 2. In the fitting procedure the 'goodness' of the fit was affected by changing the kinetic temperature. Although this had little affect upon the relative population distribution it did affect the overall quality of the fit to a degree that permitted us to obtain the rotational/kinetic temperature to within $\pm$ 15K. The resulting temperature could be checked against the temperature predicted according to the profile of the 2-0 P-branch contour which, under conditions of no overlap of the 2nd overtone emission, could be obtained unambiguously. The results from the two methods are in agreement to within the data spread. It should also be noted that in our experimental technique the minimum signal-to-noise in the first overtone spectra occurred in the highest vibrational level spectra monitored, 35-33, and was typically 25 to 1.

III. Steady State Laser Model

In order to interpret the experimentally determined vibrational distributions, we have developed a detailed kinetic model incorporating a non-Boltzmann electric energy distribution code [3] and including the dynamics of vibrational energy transfer in a multi-level system. The laser code uses a rate equation formulation and includes all $\Delta v = \pm 1$ processes for vibration-translation (VT) and vibration-vibration (VV) energy transfer, spontaneous fundamental and overtone emission processes and multi-quantum electron

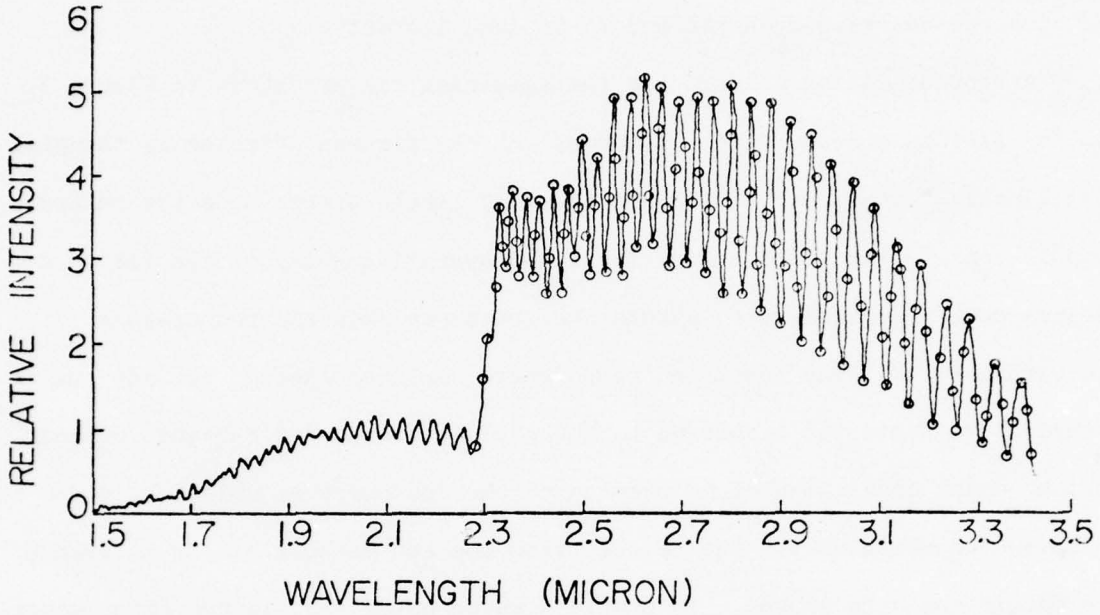


Figure 2: Experimentally observed first and second overtone spectrum for CO from a CO/He mixture (1/7) at 8.5 Torr total pressure and 155 K temperature. The points indicated are from the computer fit to the observed spectrum.

excitation and de-excitation (super-elastic) processes. The typical laser code calculation presented here includes 40 levels in CO and He as a diluent.

All electron processes are generated from the non-Boltzmann electron energy distribution code described extensively elsewhere [3]. The code solves the steady state Boltzmann equation using a defined E/N and effective vibrational temperature for each vibrational level. The electron code is directly coupled to the kinetic model so that if the vibrational temperature of CO changes enough to influence the electron energy distribution through super-elastic processes, the electron code is recalled and the rates recalculated. Although super-elastic feedback has profound effects on the high energy tail of the electron energy distribution [3], the relatively low-energy electrons responsible for vibrational excitation are essentially unaffected by changing vibrational temperature. Nonetheless the calculations presented in the following section include a fully converged super-elastic contribution to the final CO vibrational distribution.

The rate equations describing the vibrational populations, in the steady state approximation, lead to a set of coupled, nonlinear algebraic equations. These equations are numerically solved using a double precision Gauss Elimination method. The laser kinetic model and the non-Boltzmann electron energy distribution code is also available for calculating the vibrational distributions for 2 coupled diatomics with arbitrary diluents, with or without stimulated emission processes. Examples of the latter expanded code are being used to correlate $CO/N_2/He$ experiments.

Critical to the accurate prediction of the CO vibrational distribution are reliable rate coefficients and cross sections. The cross sections for

vibrational excitation by electrons used in the electron code are due to Ehrhardt, et al [4]. The other electron cross sections incorporated into electron calculation are discussed elsewhere [3].

The A-coefficients for spontaneous emission in both fundamental and overtone bands were obtained from earlier work [2].

The VT and VV rate coefficients used in these calculations are an optimized set of coefficients based on available experimental rates, theoretical predictions and analytical modeling. The basic features of the VT rate coefficients follows closely the calculations of Verter and Rabitz [6] modified by $v^{0.65}$ where v is the upper state quantum number. These VT coefficients are rather similar to those used by Rich [7] for levels $1 \leq v \leq 20$. Above about $v = 20$ the VT rates used here show a much weaker dependence on increasing v than the Rich rates [5].

The VV rate coefficients were generated using the sum of long-range and short-range potential models [8]. Adjustment of the model parameters was performed until the rate coefficients gave reasonable agreement with available experimental rates in CO as shown in Figure 3. The scaling of the short range potential model to upper vibrational states was accomplished using Morse oscillator matrix elements.

IV. Results

As will be detailed elsewhere [5], a consistent set of energy transfer coefficients, i.e. VT and VV, was determined for the CO/He system in the temperature range $125 \leq T \leq 175$K. In addition, an electron density and E/N were chosen which brought the predicted steady state CO vibrational distributions into excellent agreement with the measured distributions. A test on the consistency of the choice for the rates and the plasma parameters should consist of equally good

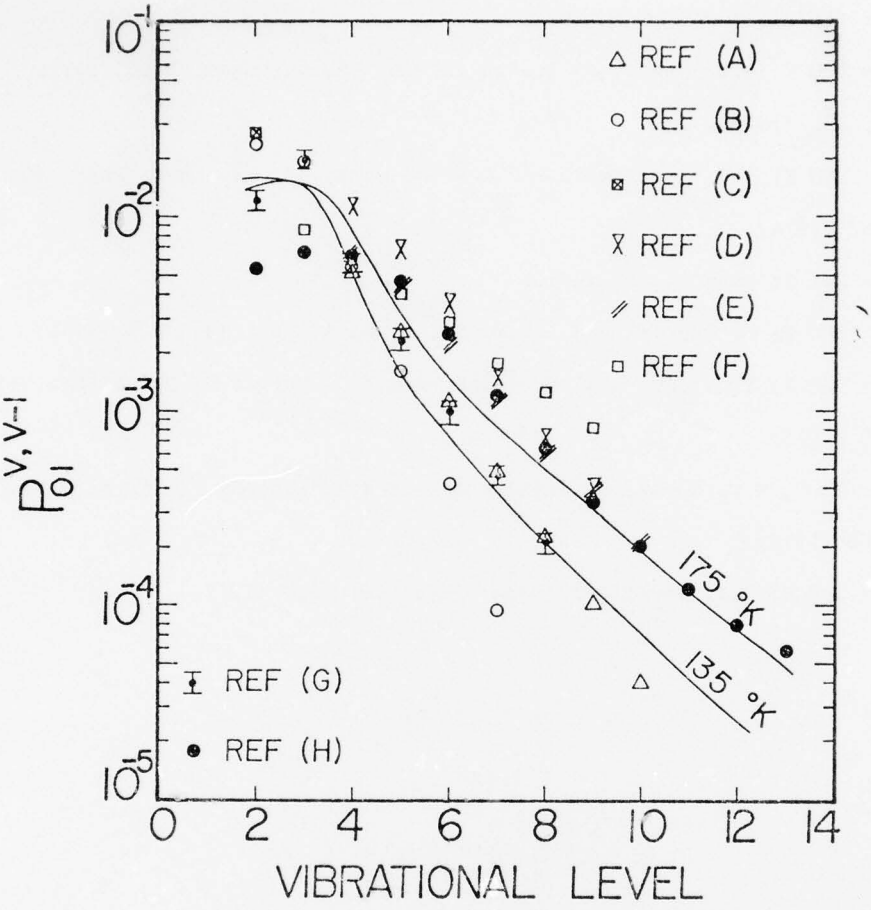


Figure 3: Calculated probabilities for VV pumping in CO at 135 and 175 K in comparison to available experimental data.

References for Figure 3:

(A) T = 100 K; I.W.M. Smith and C. Wittig, J. Chem. Soc. Fara. Trans. 69, 939 (1973).

(B) T = 100 K; H.T. Powell as quoted in R.D. Sharma, Chem. Phys. Lett. 30, 261 (1975).

(C) T = 100 K; J.C. Stephenson and E.R. Mosburg, Jr., J. Chem. Phys. 60, 3562 (1974).

(D) T = 254 K; same as (A) above.

(E) T = 300 K; G. Hancock and I.W.M. Smith, Appl. Opt. 10, 1827 (1971).

(F) T = 300 K; Y.S. Liu, R.A. McFarlane and G.J. Wolga, J. Chem. Phys. 63, 228 (1975).

(G) T = 75 K; M.C. Gower, G. Srinivasan and K.W. Billman, J. Chem. Phys. 63, 4206 (1975).

(H) T = 300 K; H.T. Powell, J. Chem. Phys. 59, 4937 (1973).

comparisons between predicted and measured distributions over a wide range of CO/He partial pressures and plasma currents. Since the plasma neutral temperature is determined from the experimental data and the CO and He partial pressures are directly measured, a model calculation can be made if the E/N and e-density are known. The voltage across the positive column and the total pressure are both measured so the E/N for the i^{th} experiment can be scaled from the "baseline" experiment by

$$\left(\frac{E}{N}\right)_i = \left(\frac{V_i}{V_b}\right)\left(\frac{P_b}{P_i}\right)\left(\frac{T_i}{T_b}\right)\left(\frac{E}{N}\right)_b \tag{1}$$

where the subscript, b, refers to the "baseline" parameters.

The electron density is related to the plasma current through

$$I = \int_0^R \int_0^{2\pi} V_D[e]\, r\, d\theta\, dr \tag{2}$$

where V_D = electron drift velocity and [e] = electron density. We can significantly simplify this relationship by assuming the drift velocity is independent of radius. Therefore, using the E/N as defined in equation (1) together with the gas partial pressures, the drift velocity can be calculated from the electron energy distribution code [3]. If the integral is then replaced by "effective" values we find

$$I = \frac{\pi}{4}\, V_D \cdot [e]_{eff} \cdot D_{eff}^2 \tag{3}$$

where [e] is assumed to be the electron density responsible for the laser excitation and D_{eff} is the effective diameter of the laser plasma responsible for transporting the current. If D_{eff} is assumed constant, the above relationship would provide a basis for scaling e-density between experiments.

Figures (4) through (6) exemplify the experimentally determined vibrational distributions in comparison to the calculated distributions based on constant D_{eff} (dashed lines). The general agreement is poor. However, when the electron density is left arbitrary, the solid lines in the above figures result.

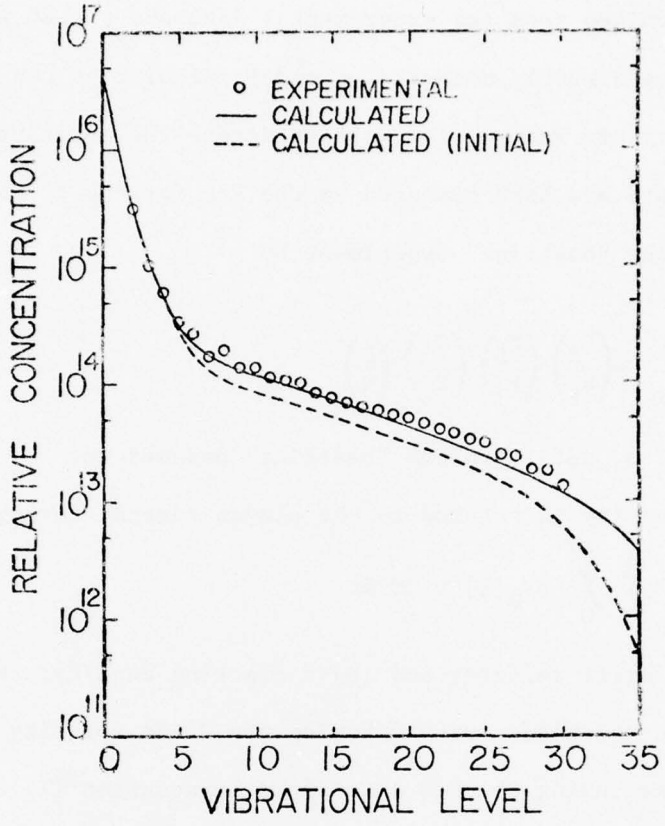


Figure 4: Steady state CO vibrational distribution for a CO/He mixture of (1/7) at 155 K. The plasma parameters used were electron density = 8.5(9) and E/N = 1.5(-16).

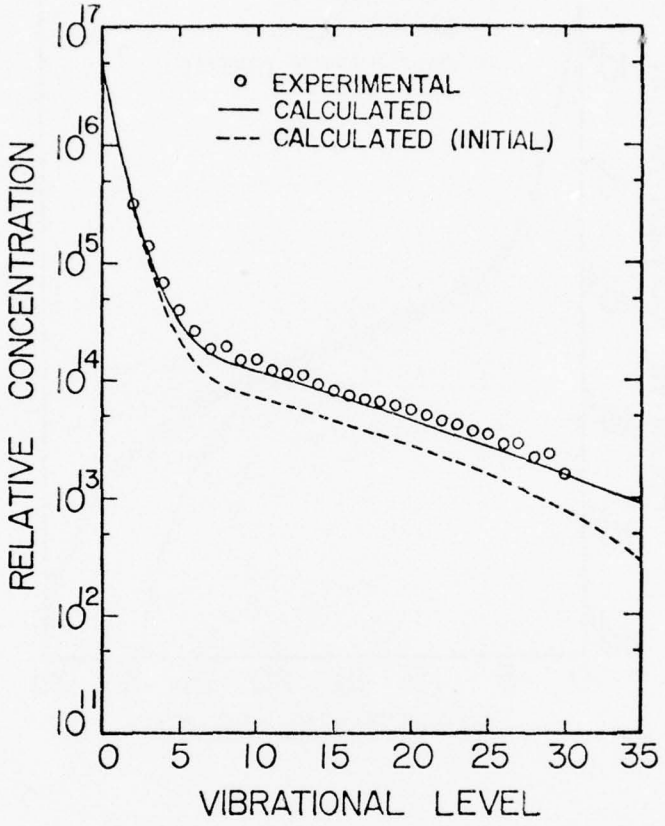


Figure 5: Steady state CO vibrational distribution for a CO/He mixture of (1/4)at 155 K. The plasma parameters used were electron density = 5.8(9) and E/N = 2.7(-16).

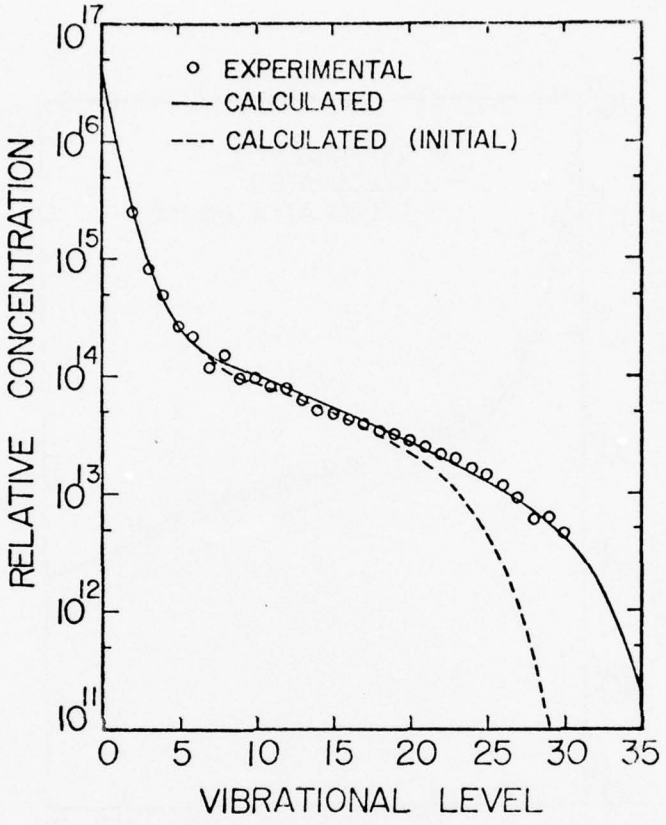


Figure 6: Steady state CO vibrational distribution in a CO/He mixture of (1/16) at 135 K. The plasma parameters used were electron density = 8.9(9) and E/N = 1.4(-16).

The agreement in all cases except Figure 6 is excellent. Figure 6 represents the experiment with the largest He partial pressure and shows a substantially larger measured population in the high vibrational states than predicted from the model. It is precisely this experimental condition, i.e. large He pressure, that should correspond to maximum cooling and lowest gas temperature. The solid line is the result of a model calculation for a 135 K temperature, 20 K below the other predictions. The agreement at this lower temperature is found to be excellent.

Four of the above runs were made under identical partial pressures of CO and He but with increasing plasma current from 5 to 15 ma. If the predicted plasma parameters from these Figures are used together with equation (3) to calculate D_{eff}, Table I results. Also shown in Table I are effective plasma diameters obtained photographically using Polaroid film. These optically derived effective diameters are in very close agreement to those obtained from the modeling calculations.

In order to show the effect of using previously accepted VT rates for CO/He, a run identical to RUN 1 (Figure 4), above, was made using the VT rates of Rich [7]. The results for this comparison is shown in Figure 7. Above about $v = 25$ where the VT rates of CO/He control the shape of the distribution the deviation is seen to be large and in disagreement with the measured values in these levels.

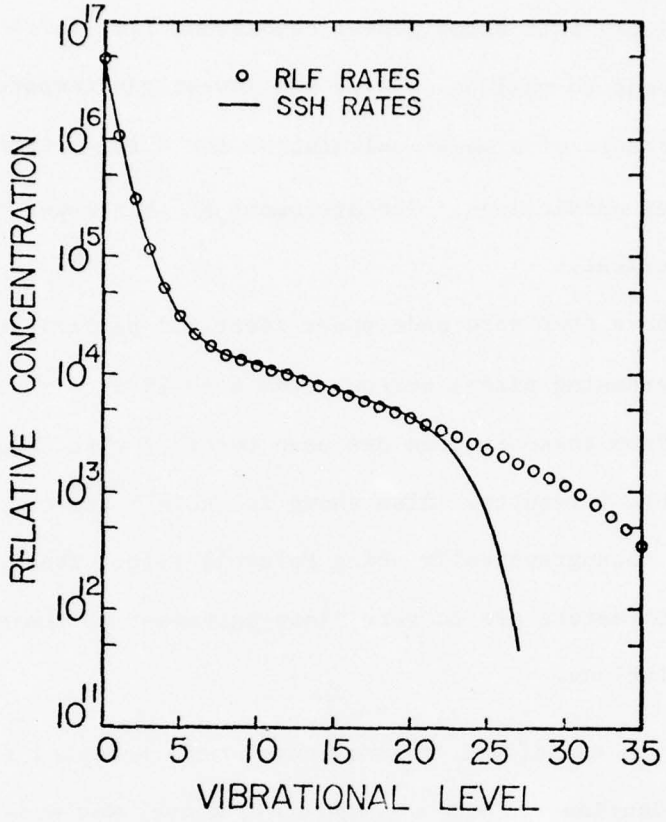


Figure 7: Comparison of steady state CO vibrational distributions calculated using the VT rates in this paper(5) and the VT rates of Rich(7) from the SSH theory. The parameters used are the same as in Figure 4.

Table I

Effective Plasma Diameter in a CO/He Laser*

I(mA)	$[e]_{eff}(cm^{-3})$	V_D(cm/sec)	$D^{\neq}_{obs}$	D_{eff}(cm)
5	8^9	$5.0^{6\dagger}$	1.0	1.0
7	1^{10}	4.5^6	1.2	1.1
10	1.3^{10}	3.7^6	1.5	1.3
15	6.5^9	5.1^6	1.8	1.9

* [CO] = 1 torr, [He] = 7 torr, D_{tube} = 2.5 cm.

≠ normalized to the 5mA observation

† $5.0^6 \equiv 5.0 \times 10^6$

Discussion

The ability to experimentally determine and analytically correlate CO vibrational distributions to high vibrational states demonstrates an important new tool to investigate the energy transfer dynamics of high vibrational states. In the experiments reported here, the agreement between experiment and predicted vibrational distributions up through v = 30 has generated a consistent set of energy transfer rates for CO/He mixtures in the temperature range near 150 K. These rate coefficients have been shown to differ significantly from past values in vibrational levels above v = 25. Further, the quantification of strong radial gradients in the electron density provide important information for use in radial diffusion models to gain greater insight into ambipolar diffusion and wall loss processes in low density CW laser systems. Additional studies involving other inert diluents (to investigate VT mass scaling effects), other wall temperatures (to investigate the temperature dependence of VV and VT rates) and additive species such as N_2 (to study N_2-CO VV pumping) and O_2[9] (to observe chemical effects in hgih states) are underway.

References

(1) C.K.N. Patel and R.J. Kerl, Appl. Phys. Lett. 5, 81 (1964); for a more recent review see M.M. Mann, AIAA 5, 549 (1976).

(2) A.J. Lightman and E.R. Fisher, Appl. Phys. Lett. 29, 593 (1976).

(3) W.L. Morgan and E.R. Fisher, Phys. Rev., in press (1977).

(4) H. Ehrhardt, L. Langhans, E. Lines and H.S. Taylor, Phys. Rev. 173, 222 (1968).

(5) E.R. Fisher, H. Rabitz and S.H. Lam, paper WA17 at 5th Conference on Chemical and Molecular Lasers, St. Louis, Mo., April (1977); manuscript in preparation.

(6) M.R. Verter and H. Rabitz, J. Chem. Phys. 64, 2939 (1976).

(7) J.W. Rich, J.A. Lordi, R.A. Gibson and S.W. Kang, Calspan Report No. WG-5164-A-3, June (1974).

(8) W.Q. Jeffers and J.D. Kelley, J. Chem. Phys. 55, 4433 (1971).

(9) E.R. Fisher and A.J. Lightman, submitted to J. Chem. Phys. (1977).

Appendix IV

"A-Coefficients for Spontaneous Emission in CO"

Allan J. Lightman and Edward R. Fisher

Appl.Phys. Letters 29, 593,1976

A coefficients for spontaneous emission in CO†

Allan J. Lightman

Department of Electrical and Computer Engineering, Wayne State University, Detroit, Michigan 48202

Edward R. Fisher

Research Institute for Engineering Sciences, Wayne State University, Detroit, Michigan 48202
(Received 6 July 1976)

Simultaneous end light emission measurements of the first- and second-overtone bands of CO have been obtained in a flowing CO-N_2-He laser plasma. Interpretation of the band structure using A coefficients from Young and Eachus show consistent agreement with observation up to $v = 26$. This agreement supports the use of these A coefficients in laser and kinetic applications.

PACS numbers: 42.60.Cz, 52.25.Ps

Fundamental to studies on improved CO laser systems and to studies using the CO laser as a probe for reacting chemical systems is an accurate knowledge of the Einstein A coefficients for the CO molecule. Since the CO molecular laser operates on fundamental transitions up to very high vibrational levels, a knowledge of the scaling of these A coefficients with increasing vibrational level is particularly important in predicting laser performance and excited CO vibrational populations.[1] Current CO laser studies[2–4] scale the A coefficients with vibrational levels using the matrix elements obtained from the cubic dipole moment function of Young and Eachus.[5] Although there has not been a serious question on the validity of this scaling procedure, we provide experimental evidence to support the use of the Young and Eachus vibration-rotation matrix elements for scaling the A coefficients up to at least $v = 26$.

As part of a program aimed at characterizing the effects of additive gases on the performance of discharge-sustained CO molecular lasers, we routinely observe spontaneous end light emission from overtone

 Copyright © 1976 American Institute of Physics

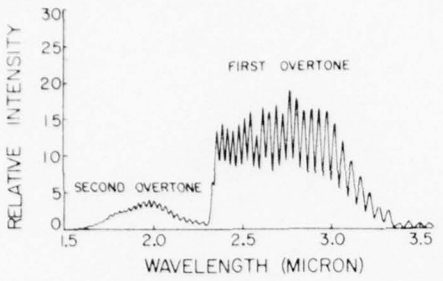


FIG. 1. Experimentally observed infrared emission from CO in a low-pressure flowing molecular laser under liquid-nitrogen cooling.

bands of CO as a means of determining the CO vibrational distributions present in the laser system. The simultaneous observation of both the first- and second-overtone emission in CO permits a consistency check on the vibrational distributions and A coefficients available for the CO molecule.

By using standard spectroscopic techniques[6–8] and the A coefficients of Young and Eachus,[5] we have determined the rotational temperature and vibrational distribution under both liquid-nitrogen and dry-ice cooling from the first-overtone band structure up to $v = 26$. From the observed second-overtone band structure, relative A coefficients corresponding to $\Delta v = 3$ transitions in CO have been determined. These experimental second-overtone A coefficients agree very well with the calculated values of Young and Eachus over the entire range of vibrational transitions from $v = 3$ to $v = 26$. This agreement supports the extensive use of these coefficients in interpreting reaction rate data[9–11] and in CO molecular laser calculations.[1–4] This letter outlines the experiments and methods used to reach this conclusion.

The infrared spectra was collected as end light emission from a flowing 15-Torr $CO/N_2/He$ mixture (1:2:10) in a laser tube 2.5 cm in diameter and 80 cm long. Typical gas velocities of 1 m/sec were used under both liquid-nitrogen or dry-ice/alcohol cooling. The cw discharge was supported by annular electrodes at

TABLE I. Relative A coefficients for vibrational transitions in CO. Calculated from the data of Ref. 5.

Upper level	Fundamental	First overtone	Second overtone
1	1.00		
2	1.92	1.00	
3	2.76	2.98	1.00
4	3.52	5.90	4.12
5	4.21	9.73	10.6
6	4.83	14.5	21.8
7	5.37	20.1	38.8
8	5.87	26.5	63.3
9	6.29	33.7	96.6
10	6.67	41.6	140
11	7.00	50.1	196
12	7.25	59.3	263
13	7.45	69.2	345
14	7.62	79.7	445
15	7.73	90.0	561
16	7.82	101	695
17	7.85	113	851
18	7.88	125	1030
19	7.84	137	1230
20	7.76	150	1460
21	7.66	162	1710
22	7.55	175	1980
23	7.35	187	2290
24	7.17	200	2630
25	6.98	213	2990
26	6.74	225	3380
27	6.49	236	3820

typically 8 kV and 10 mA. A $\frac{1}{4}$-m Jarrell-Ash monochromator with a 2.5-μ blaze grating and dry-ice/alcohol-cooled PbS photodiode located 50 cm from the discharge tube was used in collecting the spectra. Signal processing was carried out with a chopper, PAR amplifier, and either an x-y recorder or a multichannel analog tape recorder system. Analog to digital conversion was performed for data analysis. The wavelength dependence of the monochromator, detector, and recording instrumentation was calibrated by replacing the end light emission with a 900K blackbody source. The field of observation was apertured to the central 10 mm of the laser tube. For fixed mixture ratios of the laser gases, the infrared signatures were reproducible

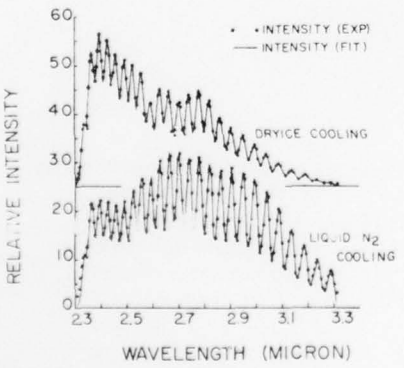


FIG. 2. Analytical fit to first-overtone CO emission under both dry-ice/alcohol and liquid-nitrogen cooling.

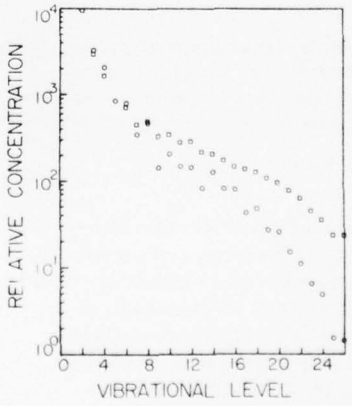


FIG. 3. CO vibrational distributions extracted from the observed first-overtone emission in Fig. 2 under liquid-nitrogen (□, T_{rot} = 135 K) and dry-ice/alcohol (○, T_{rot} = 210 K) cooling.

AD-A043 808 WAYNE STATE UNIV DETROIT MICH RESEARCH INST FOR ENGI--ETC F/G 20/5
ENERGY TRANSFER IN LASERS.(U)
JUN 77 E R FISHER, A J LIGHTMAN N00014-75-C-0284

UNCLASSIFIED NL

2 OF 2
AD
A043808





END
DATE
FILMED
9-77
DDC

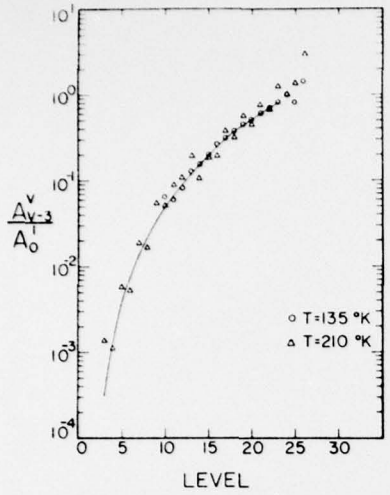


FIG. 4. Experimentally obtained second-overtone A coefficients for CO in comparison with the calculations of Ref. 5.

to better than 5%. A typical first and second overtone spectra obtained under liquid-nitrogen cooling is shown in Fig. 1. Using the data obtained and the exact values of the A coefficients,[5] the medium can be shown to be optically thin.

The rotational temperature was determined from the R branch of the $2 \rightarrow 0$ first-overtone band by a least-squares fit to a Boltzmann distribution. Using this rotational temperature and A coefficients for the CO first-overtone system as determined by Young and Eachus,[5] see Table I, the vibrational distribution was calculated by least-squares adjustment of a profile generated from the spectroscopic data of Yardley.[2] Typical spectral fits and calculated vibrational distributions are shown in Figs. 2 and 3, respectively. These distributions show the typical non-Boltzmann form expected in a discharge-supported CO system.[1,4,13]

These calculated vibrational distributions and rotational temperatures were then least-squares fitted to the observed second-overtone spectra and A coefficients were generated. A coefficients for the second-overtone transitions in CO up to $v = 26$ obtained at both liquid-nitrogen and dry-ice/alcohol temperatures are shown in Fig. 4 in comparison with theoretical values. The agreement over the entire range of accessible vibrational levels is good.

Since a consistent interpretation to both the first- and second-overtone spectra has been obtained using the A coefficients of Young and Eachus, we feel this agreement supports the use of these A coefficients in kinetic and laser applications.

†The authors acknowledge support for this study from DARPA Contract N00014-75-C-0284 monitored by ONR-Boston. The aid of Sung Won Kim, George Abraham, and Soon Sik Lim are gratefully appreciated.

[1]J.A. Lordi and J.W. Rich, Final Report on Contract No. F33615-75-C-1261, Report No. AFAL-TR-75-184, Calspan Corp., (1975).
[2]G. Abraham and E.R. Fisher, J. Appl. Phys. **43**, 4621 (1972).
[3]S.D. Rockwood, J.E. Brau, W.A. Proctor, and G.H. Canavan, IEEE J. Quantum Electron. **QE-9**, 120 (1973).
[4]M.L. Bhaumik, W.B. Lacina, and M.M. Mann, IEEE J. Quantum Electron. **QE-8**, 150 (1972).
[5]L.A. Young and W.J. Eachus, J. Chem. Phys. **44**, 4195 (1966).
[6]N.H. Bruce, S.T. Stair, Jr., and J.P. Kennealy, J. Chem. Phys. **64**, 36 (1967).
[7]G. Hancock and I.W.M. Smith, Appl. Opt. **10**, 1827 (1971).
[8]J.W. Rich and H.M. Thompson, Appl. Phys. Lett. **19**, 3 (1971).
[9]M.C. Lin and R.G. Shortridge, Chem. Phys. Lett. **29**, 42 (1974).
[10]P. Brechignac, J.P. Martin, and G. Taieb, IEEE J. Quantum Electron. **QE-10**, 797 (1974).
[11]N. Djeu, J. Chem. Phys. **60**, 4109 (1974).
[12]J.T. Yardley and J. Mol. Spectrosc. **35**, 314 (1970).
[13]N.N. Sobolev and V.V. Sokovikov, Sov. Phys.-Usp. **16**, 350 (1973).

Appendix V

"CO Vibrational Distributions in the Presence of O_2"

Edward R. Fisher and Allan J. Lightman

CO VIBRATIONAL DISTRIBUTIONS IN THE PRESENCE OF OXYGEN[+]

by

Edward R. Fisher*
Department of Chemical Engineering
Wayne State University
Detroit Michigan 48202

and

Allan J. Lightman*
Department of Electrical and Computer Engineering
Wayne State University
Detroit Michigan 48202

May 1977

[+]This research was partially supported by DARPA through ONR-Boston on Contract no. N00014-75-C-0284.

*Members: Research Institute for Engineering Sciences
Wayne State University
Detroit, Michigan 48202

ABSTRACT

Direct measurements of the vibrational distribution to $v \simeq 30$ obtained from the 1st overtone emission from CO has been made in the presence of varying amounts of O_2. These observed distributions show enhanced vibrational populations for small additions and show upper level depopulation for larger additions. Both observations support a recent plasma-kinetic model of the effect of O_2 in low pressure CO laser plasmas (1).

The effect of O_2 on CO laser performance has been extensively reported.[2-6] Until recent detailed model calculations,[1] the effect of O_2 on laser performance has been misunderstood. In this note we present direct IR measurements on the effect of O_2 on the CO vibrational distribution which supports these recent model calculations.

O_2 in small additions is known to significantly enhance laser output performance while in larger additions the laser output is known to degrade. This behavior has been related, by model calculations, to plasma-chemical processes.[1] In small additions, (i.e. $\simeq$ 10% CO), O_2^+ replaces polymer CO^+ ions as the dominant positive ion. Due to the reduced recombination rate of O_2^+, the electron density and hence the vibrational excitation rate of CO increases. In addition, the reduced E/N (electric field/total gas density) noted for small O_2 additions leads to reduced plasma heating and hence lower plasma temperatures. In larger additions, sufficient O_2 dissociation by direct electron impact is noted to produce a reduction in CO vibrational energy by CO+ O vibrational-translational (VT) relaxation. This VT relaxation, as well as other associated plasma-chemical processes,[1] leads to increased plasma heating which further reduces laser output power and efficiency. These interpretations are collaborated by the measurements and model calculations presented in this note.

For varying O_2 additions, the IR 1st overtone spectra of CO has been measured directly in a liquid N_2 cooled laser plasma.[7,8] The spectra are recorded, digitized and numerically processed to obtain CO vibrational distributions up to $v \simeq 30$. The measurements and deconvolution procedure typically leads to an accuracy of less than ±20% in the CO vibrational distribution. The magnitude of this uncertainty is directly related to water

absorption bands in the laboratory. For pure CO/He mixtures, previous work has shown quantitative agreement between measured distributions and steady state model laser calculations[8] supporting the energy transfer and electron excitation rates used in these calculations.

The steady state laser model used in these calculations incorporates a non-Boltzmann electron energy distribution code[1,9] and includes all $\Delta v = \pm 1$, VV and VT energy transfer processes. The steady state algebraic equations characterizing the vibrational distribution are solved using a Gaussian elimination procedure. The CO/He VV and VT energy transfer rate coefficients at temperatures around 150K (the temperatures encountered in this study) are an optimized set which have been shown to give agreement between measured and calculated CO vibrational distributions over a wide range of partial pressures and plasma conditions.[8.10]

In Figure 1 we show available data and calculations on vibrational relaxation (VT) of CO and N_2 by O atoms. Using the recent unpublished measurements of Lewittes, et. al as presented by Kelley and Thommarson,[11] we estimate that the relaxation time of CO + O collisions at 150 K is about 8 μsec-atm.

Calculations on the effect of O atom VT relaxation in high levels of CO requires a mass-scaling effect with increasing vibrational level over previously derived CO/He VT rate coefficients.[8] In providing this mass-scaling we have drawn on the SSH theory as developed by Lam[12] and scaled the CO/He scaling with increasing vibrational level by the ratio of reduced collision mass as appears in the exponent of the adiabaticity factor. Thus, the CO-O scaling is a factor of 2.8 larger than CO-He at v=20, 4.6 larger at v=30 and 6.4 larger at v=39. A further quantification of the effect of collision mass on VT scaling is underway.

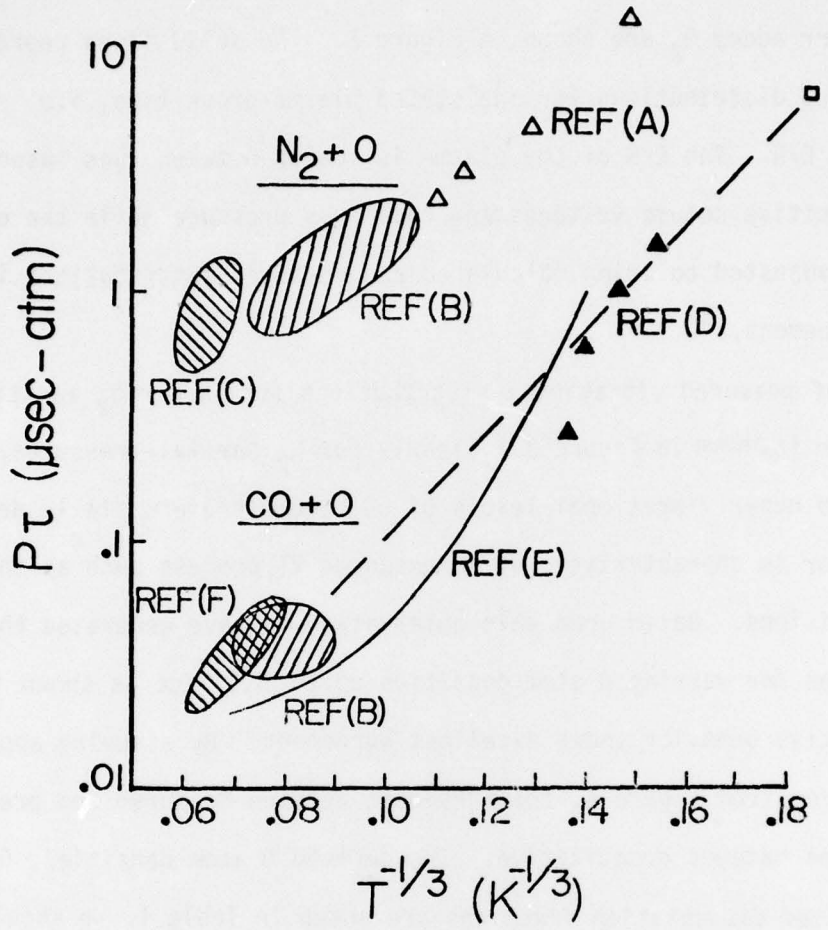


Figure 1: Vibration-translation relaxation data for O atoms on N_2 and CO.

References for Figure 1

(A) R.J.McNeal, M.E.Whitson Jr. and G.R.Cook, Chem. Phys. Letters 16, 507 (1972).
(B) D.J.Eckstrom, J. Chem. Phys. 59, 2787 (1973).
(C) W.D.Breshears and P.F.Bird, J. Chem. Phys. 48, 4768 (1968).
(D) M.E.Lewittes, C.C.Davis and R.A.McFarlane (private Communication) in reference (E) below.
(E) J.D.Kelley and R.L.Thommarson, J. Chem. Phys. 66, 1953 (1977).
(F) R.E.Center, Proc. 9th Intern. Shock Tube Symp. Stanford University Press, p. 383 (1973).

The results of measured CO vibrational distributions without O_2 and with 0.1 torr added O_2 are shown in Figure 2. The solid lines represent the predicted distributions for the stated plasma properties, i.e. electron density and E/N. The E/N of the plasma is scaled between runs based on measured positive column voltages and total gas pressure while the electron density is adjusted to bring calculated and measured distributions into optimum agreement.[8]

A set of measured vibrational distributions for larger O_2 additions up to 1 torr is shown in Figure 3. Clearly for O_2 partial pressures above 0.1 torr the upper vibrational levels of CO become preferentially deactivated. This behavior is characteristic of an enhanced VT process such as that due to CO + O collisions. Based upon this observation we have generated theoretical distributions for varying O atom densities up to 5.2^{15}/cc as shown in Figure 4. The qualitative behavior shows excellent agreement. By assuming appropriate O atom densities from Figure 4, the agreement between measured and predicted distributions becomes quantitative. The derived O atom densities, O_2 additions and calculated dissociation fractions are shown in Table 1. We should indicate that this identical behavior has been observed in the presence of N_2, suggesting that O_2 effects in $CO/N_2/He$ mixtures might be of similar origin.

Table 1

Run	O Atoms (microns)	O_2 Densities (microns)	% Dissociation
B3	10	250	2.2
B4	24	500	2.6
B5	36	1000	1.8

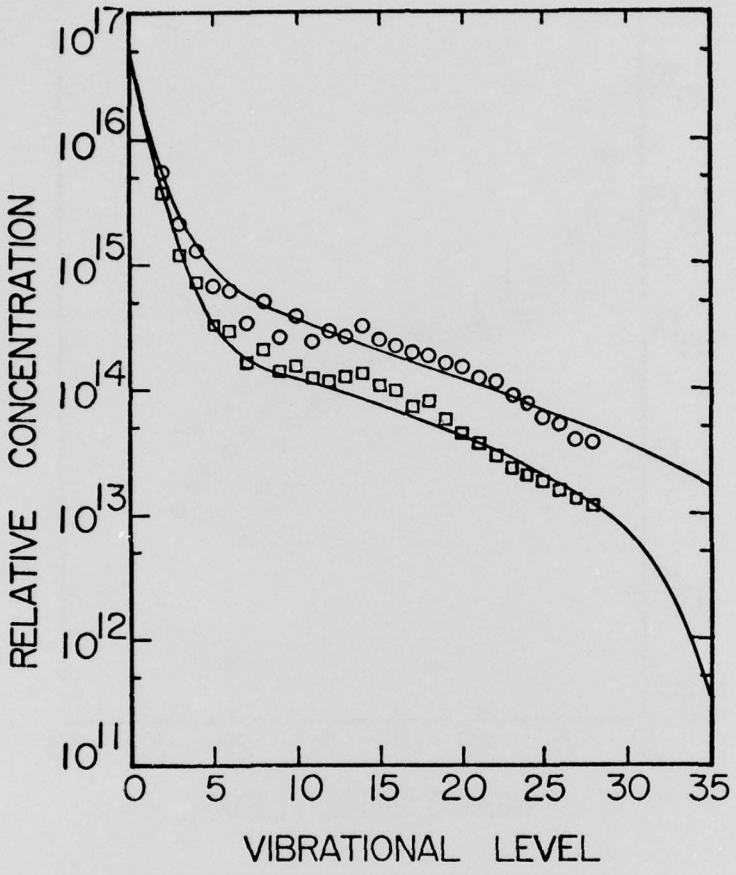


Figure 2: Measured and calculated CO vibrational distributions for a 1.5/12.5 torr CO/He mixture at 155 K with and without O_2. □ corresponds to no O_2, electron density = 1.0(10), E/N = 1.68(-16) and a current of 10 ma; O corresponds to 0.1 torr O_2, electron density = 2.0(11), E/N = 1.02(-16), and a current of 10 ma.

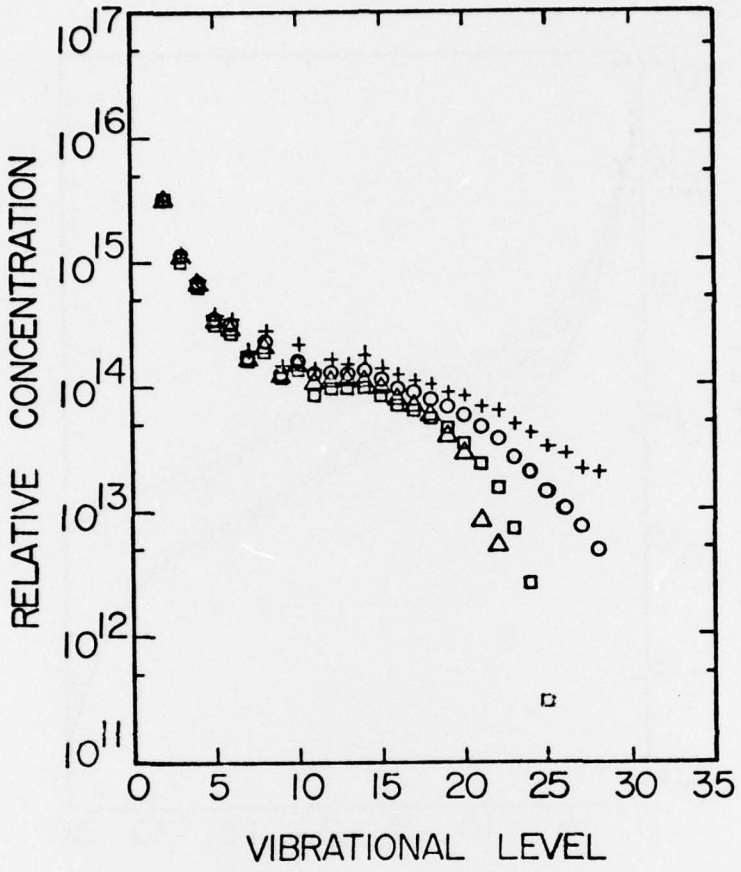


Figure 3: Measured CO vibrational distributions for a 1.5/12.5 torr CO/He mixture at 155 K and 10 ma for various O_2 additions. The symbols + / ○ / □ / △ correspond to 0/0.25/0.5/1.0 torr added O_2.

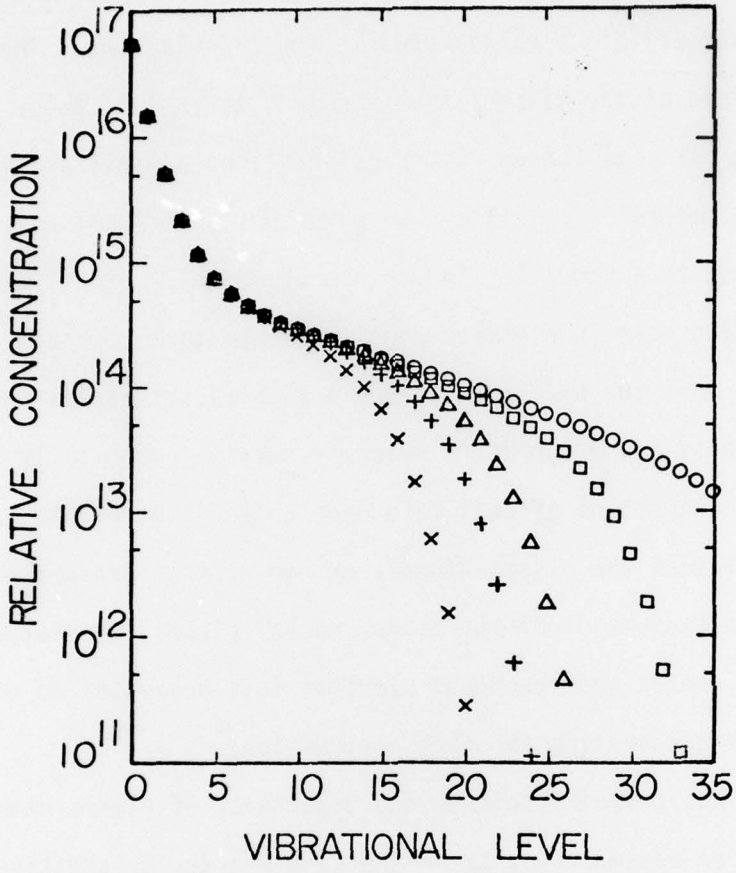


Figure 4: Calculated CO vibrational distributions for a 1.5/12.5 torr CO/He mixture at 155 K, electron density = 7.5(10) and E/N = 1.24(-16) for various O atom additions. The symbols ○ / □ / △ / + / × correspond to 0.8/8.5/26/42/83 microns of added O atoms.

Several observations emerge from the agreement between these measured and calculated CO vibrational distributions in the presence of O atoms. The first is that the general quantitative agreement is very good, lending support to the rate coefficient values used in the calculations. The second is that the magnitude of the dissociation required to explain these results is consistent with our past ion-chemistry calculations as well as the reported measurements of others[13]. Lastly, we point out that small additions of O_2 not only leads to a reduction in E/N, as observed previously, but also to a substantial increase in electron density at constant current. This observation suggests that the plasma undergoes a significant radial contraction for small O_2 additions, since the drift velocity remains essentially constant. Although large contraction effects have been noted in other plasmas[13-15], we do not yet understand the plasma-kinetic origin of this present observation. The complicating factors of polymer ions, radial plasma temperature gradients and homogeneous versus heterogeneous electron loss processes do not appear to lead to a simple explanation for this contraction.

Lastly, we would again indicate the importance of plasma-chemical processes in molecular laser plasmas and, as in the case with the O_2 additive, these processes can have a dominant influence on laser performance.

REFERENCES

(1) W.L.Morgan and E.R.Fisher, RIES Report 77-119, Wayne State University, January (1977); accepted for publication in Physical Review (1977).

(2) M.L.Bhaumik, W.B.Lacina and M.M.Mann, IEEE JQE 8, 150 (1972).

(3) T.S.Hartwick and J.Walder, IEEE JQE 8, 455 (1972).

(4) H.Keren, P.Avivi and F.Dothan, IEEE JQE 11, 590 (1975).

(5) H.Keren, P.Avivi and F.Dothan, IEEE JQE 12, 58 (1976).

(6) V.I.Volchenok, N.P.Egorov, V.N.Komarov, S.E.Kupriyanov, V.N.Ochkin, N.N.Sobolev and E.A.Trubacheev, Sov. J. Quan. Electr. 6, 1173 (1976).

(7) A.J.Lightman and E.R.Fisher, Appl Phys. Lett. 29. 593 (1976)

(8) A.J.Lightmen andE.R.Fisher, RIES Report 77-121, April (1977).

(9) W.L.Morgan and E.R.Fisher, RIES Report 74-56, August (1974).

(10) S.H.Lam, H.Rabitz and E.R.Fisher, manuscript in preparation, May (1977).

(11) J.D.Kelly and R.L.Thommarson, J.Chem.Phys. 66, 1953 (1977).

(12) S.H.Lam and H.Rabitz, J.Chem. Phys., in press (1977).

(13) S.Hatori and S.Shioda, J.Phys. Soc. Japan 40,1449 (1976).

(14) V.Yu Baranov and K.N.Ul'yanov, Soc. Phys. - Techn. Phys. 14, 176,183 (1969).

(15) K.N.Ul'yanov, Sov. Phys. Techn. Phys. 18, 360 (1973).

SECURITY CLASSIFICATION OF THIS PAGE *(When Data Entered)*

REPORT DOCUMENTATION PAGE

READ INSTRUCTIONS BEFORE COMPLETING FORM

1. REPORT NUMBER

2. GOVT ACCESSION NO.

3. RECIPIENT'S CATALOG NUMBER

4. TITLE *(and Subtitle)*

(6) Energy Transfer in Lasers.

(9) 5. TYPE OF REPORT & PERIOD COVERED

Final Technical Report,

6. PERFORMING ORG. REPORT NUMBER

7. AUTHOR(s)

(10) Edward R. Fisher and Allan J. Lightman

8. CONTRACT OR GRANT NUMBER(s)

(15) N00014-75-C-0284 new

9. PERFORMING ORGANIZATION NAME AND ADDRESS

Research Institute for Engineering Sciences
Wayne State University
Detroit, Michigan 48202

10. PROGRAM ELEMENT, PROJECT, TASK AREA & WORK UNIT NUMBERS

11. CONTROLLING OFFICE NAME AND ADDRESS

(11)

12. REPORT DATE

June 1977

13. NUMBER OF PAGES

109

14. MONITORING AGENCY NAME & ADDRESS *(if different from Controlling Office)*

Office of Naval Research
495 Summer Street
Boston, Mass. 02210

(12) 109p.

15. SECURITY CLASS. *(of this report)*

Unclassified

15a. DECLASSIFICATION/DOWNGRADING SCHEDULE

16. DISTRIBUTION STATEMENT *(of this Report)*

Approved for Public Release, Distribution Unlimited

17. DISTRIBUTION STATEMENT *(of the abstract entered in Block 20, if different from Report)*

18. SUPPLEMENTARY NOTES

The findings in this report are not to be construed as an official Department of the Navy position, unless so designated by other authorized documents.

19. KEY WORDS *(Continue on reverse side if necessary and identify by block number)*

Molecular laser studies, CO plasma chemistry, energy transfer processes in CO

20. ABSTRACT *(Continue on reverse side if necessary and identify by block number)*

This final report details plasma-chemical and energy transfer studies carried out at the RIES. Experimental and analytical research has been aimed at understanding additive effects in discharge supported molecular laser systems, particularly the CO laser system. Extensive numerical model codes have been developed and applied to the CO system with considerable success. Experiments in our laboratories have provided important information on high lying vibrational states in CO, in agreement with model predictions. Collaborative studies between RIES and Princeton University on the behavior of vibrational distributions under strongly pumped conditions is outlined.

DD FORM 1 JAN 73 1473 EDITION OF 1 NOV 65 IS OBSOLETE

405399

SECURITY CLASSIFICATION OF THIS PAGE *(When Data Entered)*